

MAY 14 1942

ACR May 1942

NATIONAL ADVISORY COMMITTEE FOR AERONAUTICS

# WARTIME REPORT

ORIGINALLY ISSUED  
May 1942 as  
Advance Confidential Report

HIGH-SPEED TESTS OF RADIAL-ENGINE NACELLES

ON A THICK LOW-DRAG WING

By John V. Becker

Langley Memorial Aeronautical Laboratory  
Langley Field, Va.

FOR REFERENCE

NOT TO BE TAKEN FROM THIS ROOM

# NACA

WASHINGTON

NACA WARTIME REPORTS are reprints of papers originally issued to provide rapid distribution of advance research results to an authorized group requiring them for the war effort. They were previously held under a security status but are now unclassified. Some of these reports were not technically edited. All have been reproduced without change in order to expedite general distribution.

L - 229

NACA  
LANGLEY MEMORIAL AERONAUTICAL  
LABORATORY  
Langley Field, Va.

NATIONAL ADVISORY COMMITTEE FOR AERONAUTICS

ADVANCE CONFIDENTIAL REPORT

HIGH-SPEED TESTS OF RADIAL-ENGINE NACELLES

ON A THICK LOW-DRAG WING

By John V. Becker

SUMMARY

Tests were made in the 8-foot high-speed wind tunnel to determine the drag characteristics of several conventional types of radial-engine nacelle on a low-drag airfoil. Models, 1/8 full scale, simulating installations of the Wright 3350 engine in heavy bomber types were employed.

The drag coefficients of nacelles incorporating cowlings-nose shapes shown by previous tests to be efficient and afterbodies of adequate length were of about the same magnitude as commonly obtained for comparable installations on conventional wings. Nacelles that had high drag coefficients at low speeds suffered from large increases in drag with increasing Mach number. For the best arrangements tested, however, no serious increases occurred in drag coefficient within the limit of the tests, which covered a range of Mach numbers up to 0.55.

INTRODUCTION

In the design of recent multiengine airplanes there has been considerable conjecture regarding the drag and interference of radial-engine nacelles on low-drag types of wing. Little data obtained under the necessary low-turbulence testing conditions have been available.

The present test program was an outgrowth of tests in the NACA 8-foot high-speed wind tunnel of a 1/8-scale model bomber-type airplane in which an unusually high drag occurred with the original nacelles on the low-drag wing. Tests of improved nacelles showed that the excessive drag was due to a poorly shaped cowlings and a

very blunt afterbody shape rather than to serious adverse interference with the low-drag wing.

The present investigation included tests of further modifications to the nacelle of the airplane tested and tests of several other typical nacelles of varying size, location, and shape detail. The principal aim was to provide general information of immediate engineering interest on several types of nacelle rather than to study in detail any isolated variables. The models tested were 1/8-scale representations of installations of the Wright 3350 engine in heavy bombers. A pusher arrangement was included in the program. This type has the advantage of eliminating the increase in frictional drag of the wing due to the slipstream disturbance. Details of the pusher installation of the Wright 3350 engine were designed in cooperation with the NACA power-plant installation group.

In addition to the usual force data, pressure-distribution data were obtained at the wing-nacelle junction of each model. In order to provide data frequently requested for structural design, the pressure distribution over the NACA cowling-C profile (reference 1) of one of the models was measured at high angles of attack.

The work was done by the NACA at the Langley Memorial Aeronautical Laboratory, Langley Field, Va.

#### SYMBOLS

$V$	free-stream velocity
$\rho$	mass density of air in internal flow
$\rho_0$	free-stream density
$q$	free-stream dynamic pressure ( $1/2 \rho_0 V^2$ )
$Q$	volume rate of flow through duct at density $\rho$
$F$	maximum cross-sectional area of nacelle

- $A_e$  maximum cross-sectional area of engine (18.4 sq ft for Wright 3350 engine)  
 $a$  velocity of sound in air  
 $M$  Mach number,  $V/a$   
 $p$  pressure  
 $P$  pressure coefficient  $(P_{local} - P_{stream})/q$   
 $\alpha$  angle of attack of wing  
 $C_{DF}$  external drag coefficient of nacelle  
 $[(\text{total drag of combination}) - (\text{drag of wing at same angle of attack}) - (\text{drag calculated from internal losses})]/q$

#### APPARATUS

The tests were conducted in the 8-foot high-speed tunnel, in which the turbulence level is considered to be sufficiently low to permit significant results to be obtained with models incorporating low-drag airfoils.

Wing.— The wing on which the nacelles were installed was a 1/8-scale model of a wing of NACA low-drag section designed for the airplane tested. The portion of the wing represented included most of the left panel and a small length of the right panel. When both inboard and outboard nacelles were represented, the nacelles were equidistant from the center line of the tunnel. The airfoil section employed at the root was the NACA 65,2-221 and at the tip, the NACA 66,2X-416. The inboard nacelle was located 21.04 inches from the root at a station where the wing chord was 20.63 inches and the thickness ratio was 20.7 percent. The outboard nacelle was situated 45.96 inches from the root at a station where the wing chord was 16.65 inches and the thickness ratio was 19.9 percent.

The wing was set at  $3^\circ$  angle of incidence to the thrust lines of all of the nacelles except the pusher type (nacelle 5), for which the angle was  $2^\circ$ . Angles of attack shown in this report are those of the wing.

Cooling-air flow.— All the nacelles were tested with internal air flow corresponding to the estimated requirements of the Wright 3350 engine, and the internal pressure drops were simulated as closely as possible by means of perforated plates. The values assumed for the flow characteristics were as follows for full-throttle operation at 400 miles per hour and at 28,000 feet altitude:

	(cu ft/min)
Engine cylinder cooling . . . . .	35,000
Accessory cooling and charge air . . . . .	<u>35,000</u>
Total	70,000

The value assumed for the pressure drop was 8 inches of water for the engine baffle and also for the accessory systems. The nondimensional pressure-drop ratio was, therefore,

$$\frac{\Delta p}{q} = \frac{8 \times 5.2}{1/2 \times 0.00238 \times 0.448 (400 \times 1.47)^2} = 0.23$$

The perforated resistance plates were designed to produce this pressure-drop ratio at the required rate of internal flow. The internal mass-flow rate is conveniently expressed nondimensionally as the ratio  $\rho Q / \rho_0 A_e V$ . For the assumed flow condition, the value of  $\rho Q / \rho_0 A_e V$  is 0.11. The outlet openings were designed to produce this flow ratio, and it will be noted that the measured rates of flow closely approach the design value except, of course, in those runs in which the outlet-opening area was reduced.

Original nacelle design.— The original nacelle tested was a 1/8-scale model of a 72-inch-diameter circular-section installation in which the engine was located in the upper part of the nacelle and the accessory air was carried underneath and around the sides of the engine. The nacelle was designed by a manufacturer and was submitted to the NACA for tests in the 8-foot high-speed wind tunnel. The cowl profile was unsymmetrical in side view with a relatively sharp edge at the top of the cowl. The blunt afterbody fairing was the result of enclosing two 56-inch wheels in a low nacelle terminating at the trailing edge of the wing.

The model was tested with internal flow representing only cylinder cooling.

The nacelle ordinates measured as in figure 1 are given in table I. Sketches of each nacelle are included in table II.

Nacelle 1.— Nacelle 1 has the same depth at each afterbody station as the original design. A much improved afterbody fairing was obtained by making the nacelle symmetrical about its center line. The nacelle was also raised above the original low position so that its center line passed through the trailing edge of the wing. The original cowl nose was supplanted by cowl profile C of reference 1. In other respects nacelle 1 was similar to the original design.

Nacelle 1A.— In order to compare the merits of the central position of nacelle 1 with a low position of efficient aerodynamic shape, the original low afterbody was extended, as shown in figure 1 and in tables I and II. Nacelle 1A was otherwise identical with nacelle 1.

Nacelle 2.— Nacelle 2 was included to indicate the effects of an improved nose shape. The conventional C-type cowl of nacelles 1 and 1A was replaced by an arrangement designated NACA cowl E. This arrangement embodies a hollow spinner through which all the required air is admitted at a velocity of about  $0.4V$  for the high-speed condition. The external lines of the spinner are obtained from nose B of reference 2. The air for the auxiliaries was carried by means of two ducts over and under the resistance plate representing the engine. After passing through a resistance simulating the accessory pressure drops, the air was exhausted through an outlet at the top of the nacelle. The engine cooling air was exhausted at either side of the nacelle. The auxiliary air ducts required a bump in the side-view contour on top and bottom of the nacelle. In plan view the nacelle contour was a continuation of the nose B contour (reference 2) of the spinner. The afterbody of nacelle 2 was identical with that of nacelle 1 except for the addition of the auxiliary air outlet. The outlet openings of nacelle 2 and all subsequent models were undercut below the basic profile of the nacelle for some distance back of the actual opening, as recommended in reference 2. Details of a typical outlet are given in

figure 2. As originally planned, the propeller blade shanks within the outer spinner of cowling E in an actual installation were to be covered by fairings extending between the outer spinner and an inner spinner that covered the hub. The fairings were intended to aid in ground and climb cooling and to operate at zero lift in the high-speed condition. On the model, this high-speed condition was simulated by setting the three-blade fairings with their axes parallel to the thrust line, since the model spinner did not rotate. (See fig. 3.)

Nacelle 2A.— The opening on top of nacelle 2 was faired over for model 2A in order to indicate the effect of the opening.

Nacelle 2B.— Nacelle 2B was tested to permit evaluation of the improved nose shape on a low nacelle. The nacelle is a combination of the nacelle 1A afterbody and the nacelle 2A forebody.

Nacelle 2C.— Nacelle 2C was the same as nacelle 2B except for enlarged (deepened) outlet openings. (See fig. 3.)

Nacelle 3.— The large size of the nacelles thus far described (72 in. diameter, full scale) was necessary to permit enclosure of the landing gear. Nacelles 3 to 5 and their modifications are types in which the maximum cross-sectional dimensions were made as small as possible from considerations of only the engine size and the cooling-air requirements.

Nacelle 3 was elliptical in cross section. The depth, 60 inches full scale, was limited by the engine diameter, and the width, 72 inches, was chosen in order to allow enough space on either side of the engine for supplying air to the accessories. The C-cowling contour of reference 1, derived for a 4.50-inch radius, was maintained around the nose. The maximum cross section was a true ellipse as were the afterbody sections. The line of symmetry of the nacelle passed through the trailing edge of the wing. Four outlets were provided, one on either side for the engine cooling air and one each on the top and on the bottom for the accessory air.

Nacelle 3A.— The bottom outlet of nacelle 3 was faired over to form nacelle 3A.

Nacelle 3B.— In order to evaluate the effect of shortening the afterbody, nacelle 3B was designed with the afterbody terminating at the 50-percent-chord station of the wing. It was otherwise identical with nacelle 3A.

Nacelles 3C and 3D.— Nacelles 3C and 3D were identical with nacelle 3 except that the side outlets were closed and faired over on nacelle 3C and the top and bottom outlets were closed and faired over on nacelle 3D.

Nacelle 4.— Nacelle 4 represents about the minimum size (60 in. diameter, full scale) that will house the Wright 3350 engine. No provision was made for accessory air on the model. Either scoops or wing inlets would be necessary. The C-cowling contour (reference 1) was derived for the maximum radius of the nacelle. In side view the afterbody contour is identical with that of nacelle 3B. The cross sections were circular throughout.

Nacelle 5.— Nacelle 5, the pusher type (figs. 1 and 4, and tables I and II), was designed around the installation shown in figure 5. All the required internal air flow was admitted at the nose of the nacelle at an inlet velocity of about  $0.4V$ . The external nose profile was that of nose B of reference 2 carried back as far as the leading edge of the wing. The leading edge of the nacelle was extended ahead of the wing by about 13 percent of the chord in order to prevent interference effects due to the low pressures on the forward part of the wing at high angles of attack. The vertical position of the nacelle was adjusted to allow equal duct space above and below the wing for the engine cooling air. The ducts (fig. 5) leading to the oil coolers, intercoolers, and superchargers were simulated on the model by means of a single duct in each wing terminating in an outlet opening on either side of the nacelle (fig. 4(b)). The right opening was placed close to the nacelle in order to permit a comparison of the interference effects at that location with the effects at the location of the left outlet further outboard. The internal flow was divided approximately as follows: 50 percent through the nacelle and 25 percent through each wing duct.

Nacelle 5A.— Nacelle 5A was the same as nacelle 5 except that the right outlet was closed.

Nacelle 5B.— The fillet sketched in figure 1 was added to nacelle 5A to make nacelle 5B.



Nacelle 5C.— Nacelle 5C was the same as nacelle 5 except that the left outlet was closed.

Outboard nacelle.— The outboard nacelle was the manufacturer's design for the airplane. It was similar to the original inboard nacelle previously described except that the C-cowling contour was employed.

Pressure measurements.— Pressure-distribution data were obtained on the cowling-C profile of nacelle 3 by means of flush orifices on the top and the side of the cowling. Pressures in the wing juncture of each nacelle were measured by small portable static tubes. The tubes were aligned parallel to the flow direction as indicated by tufts. The rate of internal flow and the internal pressure drops were measured by surveys at several stations in each outlet opening, taken with rakes of total-pressure and static-pressure tubes.

## TESTS

Force tests.— The lift and drag characteristics of the wing alone and in combination with each of the nacelles were measured for the following conditions:

(1) From  $\alpha = -1^\circ$  to  $8^\circ$  at  $M = 0.26$

(2) From  $M = 0.17$  to  $0.55$  at  $\alpha = 0^\circ$  and  $2^\circ$

( $C_L \approx 0.13$  and  $0.38$ )

Tests of inboard nacelle 1A were also made in the presence of the outboard nacelle for the listed conditions.

Pressure measurements.— Pressure data at the wing-nacelle junctures were obtained for all configurations at  $M = 0.33$  for angles of attack of  $-1^\circ$ ,  $2^\circ$ , and  $6^\circ$ . Pressure distributions over cowling C of nacelle 3 were obtained through an angle-of-attack range of  $-1^\circ$  to  $16^\circ$  at  $M = 0.26$ , and from  $-1^\circ$  to  $3^\circ$  for  $M = 0.17$  to  $0.55$ . Surveys of static and total pressure were made in each outlet opening in order to determine the internal flow quantity, the pressure drop, and the internal drag.

Drag of the wing.— A special effort was made throughout the tests to keep the wing surface ideally smooth and fair. The drag of the wing alone was measured five times during the tests and was found to deviate from the original values by not more than  $1\frac{1}{2}$  percent (about 4 percent of average nacelle drag increment).

## RESULTS

Reduction of data.— The drag increments due to the nacelles are given in the form of coefficients based on the nacelle frontal area. The calculated drag corresponding to the momentum loss of the internal flow has been deducted from the total drag increment, and the remaining external drag increment is presented in this report. Through the use of this parameter the effect of changes in external shape, with which this investigation is mainly concerned, can be studied directly. Drag-coefficient changes associated with the internal flow are accounted for. The values of the internal-drag increments calculated from the measured internal-flow characteristics by the method of reference 2 are shown in table III for each nacelle. If it is desired to obtain the total nacelle drag-coefficient increment, the values given in this table may be added to the external-drag values shown in the subsequent figures of this report. The total drag-coefficient increment is of interest only at the design speed, because lower speeds would require larger exit openings and higher internal drag.

Tests with fixed transition on the wing.— In previous tests of nacelles on conventional wings, it has been found desirable to fix the transition point near the leading edge of the wing in order to make the boundary-layer conditions correspond to those of flight. For the low-drag type of wing, however, the full-scale flight transition location is not definitely known and therefore cannot be simulated in model tests. In addition, it has been found that the methods used to fix the transition location bring about a type of transition considerably different from the type that occurs naturally on a smooth low-drag wing. A few runs were made during the present investigation with the transition fixed on both the upper and the lower surfaces of the wing at the 15-percent-chord station in order to determine the nacelle drag for this extreme of the boundary-layer condition. It was found that the nacelle

drag was of the order of half the value obtained on the smooth wing. Because the fixed transition data were of doubtful significance and indicated very low nacelle drags, no further fixed-transition tests were made. All the data presented in this report were obtained with the smooth wing.

Force-test data.— The external drag coefficients of the nacelles, grouped according to type, are shown in figures 6 to 9 as functions of  $M$  and  $\alpha$ . The small interference drag between the inboard and the outboard nacelles is shown in figure 10. A comparison of the drag of nacelles typical of each type is made in figure 11. Table II affords a comparison of all the nacelles. In addition to the drag coefficients, the drag in pounds at 25,000 feet altitude and at  $M = 0.50$  is tabulated to show the over-all drag changes including the effect of changes in the nacelle frontal area. Favorable interference effects associated with the outlet flow are shown in figures 12 and 13. Figure 14 shows the lift coefficients of the wing-nacelle combinations.

Pressure data.— The pressure distributions over cowl-  
ing C (nacelle 3) are presented in figures 15 and 16. These data are given in considerable detail, particularly as regards angle-of-attack range, because a number of requests have been received for data applicable to structural design at high angles of attack.

Pressure distributions at the juncture of the wing and nacelle 3 are shown in figure 17. These results were typical of the juncture pressures obtained with the other nacelles.

## NACELLE DRAG

Vertical location.— In a series of preliminary tests not described in this report, it was found that about two-thirds of the large drag reduction that occurred when the manufacturer's original nacelle was replaced by the centrally located nacelle 1 (table II and fig. 6) was the result of raising the nacelle to the central position. The rest of the reduction in drag occurred through the use of cowl-  
ing C. A separated flow condition that existed over the original afterbody did not occur with nacelle 1

because of the greatly improved afterbody shape made possible by the central location. The same result was obtained by lengthening the afterbody of the original low nacelle. (Cf. nacelles 1 and 1A, 2A and 2B of table II and figs. 6 and 7.) The nacelle in the low position with the extended afterbody gave lower drags than the nacelle in the central position for angles of attack greater than  $5^\circ$  (figs. 6(c) and 7(c)). It thus appears that the central location offers no advantage except in the cases where a large nacelle must be terminated near the trailing edge.

Extended afterbody.— The adverse pressure gradient over a nacelle afterbody is superimposed on the adverse gradient of the wing if the nacelle is terminated at or near the trailing edge of the wing. The resulting pressure gradient will be more severe than for either wing or nacelle alone and separation effects will be encouraged. This result is particularly true of low-drag wing sections that commonly have steeper adverse gradients than conventional sections and is one of the reasons that nacelle drags on low-drag wings tend to be greater than on conventional wings. The difficulty can be circumvented by extending the nacelle afterbody, a procedure which not only moves the adverse gradient on the nacelle away from that of the wing but which also reduces the magnitude of the gradient on the nacelle. The beneficial effect in the case of nacelles 1A and 2B was very large, as previously shown, because of the critically poor shape of the original nacelle. In this instance a nacelle extension of only 15 percent of the wing chord was sufficient to prevent serious separation. The amount by which the nacelle should be extended is a function of a large number of variables; tests to determine the optimum length in individual cases will probably be required.

Cowling shape.— The reduction of the drag of the original nacelle by one-third through the use of cowling-profile C (reference 1) was due to elimination of local separation of the flow over the top of the original blunt profile. A comparison of cowling C with the high-speed cowling E showed that the minimum drags at moderate speeds were about the same. (Cf. nacelle 1 with 2A or nacelle 1A with 2B, table II.) At Mach numbers beyond 0.62, however, the drag with cowling C has been found to increase precipitously (reference 1) owing to the compressibility burble; whereas the drag of cowling E remains low up to Mach numbers of the order of 0.70 to 0.80, depending on

the magnitude of the protuberances due to the accessory air ducts around the engine. In the absence of the protuberances, no pressure peak occurs on the E-cowling profile (reference 2).

The drag with cowling E was considerably less than with cowling C at the higher angles of attack. (Cf. nacelles 1 and 1A with 2 and 2A in figs. 6(c) and 7(c).) The entrance and duct losses with cowling E were found to be negligible throughout the entire range of angles of attack, indicating that higher front pressures would be available with cowling E than with cowling C, for which the entrance losses are appreciable at the higher angles. Unfortunately, this result cannot be translated directly into flight performance because the effect of the propeller-shank fairings with a rotating propeller is not included. The entrance and duct losses in the pusher arrangement were likewise found to be negligible throughout the angle-of-attack range. This design also employed the cowling E profile at the entrance.

Nacelle size.—Nacelles smaller than 72 inches in diameter are feasible where provision for large wheels is not required; for example, in flying boats or in the outboard nacelles of four-engine landplanes. Large drag reductions can be made partly as a result of the reduced cross-sectional and wetted areas and partly through the reduced interference drag of the smaller nacelles. The 72- by 60-inch elliptical nacelle has 83 percent of the frontal area of the 72-inch-diameter model but only 54 percent of the drag. (See nacelle 3 of table II. The drag coefficients shown in table II and in fig. 8, being based on frontal area, show only the changes due to variations in interference effects; hence, a column is included in table II showing the drag of each nacelle in pounds for a typical operating condition.) The reduced interference effects probably result from the fact that a larger proportion of the wetted area of the smaller nacelle is covered by the wing. The improved afterbody fairing and increased fineness ratio are probably also beneficial. An afterbody extending only to the 50-percent-chord station of the wing resulted in about the same drag as the longer afterbody. (Cf. nacelles 3A and 3B, fig. 8, and table II.)

Further decrease in the nacelle dimensions to 60 inches diameter, the minimum size that will enclose the Wright 3350 engine, permitted still further reductions in the nacelle drag (nacelle 4, fig. 8, and table II). This

model had no provision for the introduction of auxiliary air, however, and it is not likely that any net saving over nacelle 3 would occur if scoops were added or if any inlets were employed.

Pusher nacelle.— With the pusher-nacelle arrangement it was possible to admit all the required air through an efficient inlet opening at the nose of the nacelle (cowling-E profile, nose B of reference 2) and, at the same time, employ the minimum possible diameter of 60 inches. Sufficient space was available for efficient ducts to the intercoolers and turbosuperchargers carried in the wing on either side of the nacelle (fig. 5). This nacelle had the lowest drag of any model tested. (See nacelle 5, fig. 9, and table II.) The drag at  $M = 0.50$ , for the flow condition corresponding to 25,000 feet altitude, was 33 percent of the drag of nacelle 1 and 61 percent of the drag of the elliptical nacelle 3. As previously mentioned, the pusher arrangement would not suffer as would the tractor type from increases in wing drag due to disturbance of laminar flow on the wing by the slipstream.

Interference between inboard and outboard nacelles.— In the minimum drag condition the interference was negligible (fig. 10(a)). At high angles of attack a favorable interference effect occurred (fig. 10(c)), probably as a result of reduction of the separated flow over the blunt afterbody of the outboard nacelle.

Comparison with conventional wing.— Drag results previously obtained for nacelle 1A on a wing of mere conventional section are unfortunately not directly comparable with the present results: first, because the thickness of the conventional wing was greater (22.7-percent-thick section) and, second, because the data with the conventional wing were measured in the presence of a large fuselage. The results of reference 3, although not strictly comparable with the results presented herein because a wing of 13-percent thickness ratio was employed, permit a comparison of good conventional nacelles at identical values of the ratio of nacelle diameter to wing thickness. The following table compares the minimum external drag coefficients of these tests with those obtained in reference 3 at approximately the same Reynolds number. It is pointed out that the comparison tends to be unfavorable to the low-drag-wing data in that the Mach number was 0.30 and the lift coefficient 0.4 in the present tests as compared with a Mach number of 0.08 and a lift coefficient of 0 in the full-scale-tunnel tests.

Nacelle diameter Wing thickness	$C_{D_F}$		
	Nacelle on conventional wing	Nacelle on low-drag wing	
			Nacelle
2.10	0.055	0.067	1
2.10	.055	.070	1A
2.10	.055	.058	2
1.75	.050	.049	3
1.75	.050	.043	4
1.75	.050	.041	5

This comparison shows that, in spite of the factors tending to increase the nacelle drag on a low-drag wing (disturbance of the laminar flow on the wing by the nacelle and increased separation tendencies), the drag of suitable nacelles is not greatly different from the drag of similar nacelles on a conventional wing.

Effect of an operating propeller.— The drag coefficients of the tractor nacelles on the low-drag wing would be somewhat increased if an operating propeller were present because the propeller would create a disturbance of the laminar flow on the wing. An estimate of this effect for the original nacelle on the 20.7-percent-thick wing can be made on the assumption that the boundary-layer flow changes from the laminar to the turbulent type over 40 percent of the airfoil surface as a result of the propeller action. The dimensions used and the calculation are as follows:

Propeller diameter, feet . . . . .	16 $\frac{1}{2}$
Nacelle diameter, feet . . . . .	6
Wing chord, feet . . . . .	13 $\frac{3}{4}$

Increase in section drag coefficient of wing due to propeller action,  $\Delta c_d$  . . . . . .0020

$$\Delta C_{D_F} = \frac{(0.0020)(\text{wing area exposed to slipstream})}{\text{nacelle cross-sectional area}}$$

$$= \frac{0.002 \left[ \left( 16\frac{1}{2} - 6 \right) \left( 13\frac{3}{4} \right) \right]}{28.2}$$

$$= 0.010$$

This value represents about 13 percent of the drag of the 72-inch-diameter nacelles and about 31 percent of the drag of the 60- by 72-inch nacelle.

Variation with Mach number.— Figure 11 shows that the drag of the original nacelle increased very rapidly with Mach number, probably because the flow separation becomes more intense as the speed increases. If the nacelle drag coefficient is high at low speeds, a much higher value may be expected at high speeds. If the drag is small at low speeds, however, indicating satisfactory flow conditions, no serious increases with speed occur until the critical compressibility speed is reached. It will be noted in figure 11 that the maximum test Mach number, 0.55, was considerably lower than the critical Mach number of any of the nacelles (cowling C, critical  $M = 0.62$ ).

Beneficial effects of air outlet.— The outlet openings on nacelles 2 to 5 were designed in accordance with the suggestion of reference 2 that the outlet flow should cause a minimum of disturbance to the static pressures over the basic body, which condition requires that the outlet profile be cut below the basic body profile for some distance back of the actual opening (fig. 2). It was found in several cases that the drag was less when the outlets were open than when faired over. The top outlet of nacelle 2 had a large favorable effect (see fig. 12), apparently the result of decreasing a local separation on the upper wing-nacelle juncture. The top and bottom outlets of nacelle 3 had a similar effect, but the side outlets, located in the positive pressure field of the wing, added somewhat to the drag. (Cf. figs. 8 and 13.) Alternate fairing over of the wing outlets of nacelle 5 (fig. 12) showed that



both had a favorable effect. The left outlet was more effective than the right, which was located in the wing-nacelle juncture (fig. 4(b)).

#### EFFECT OF NACELLES ON LIFT

At a given angle of attack, all the nacelles tested decreased the lift when added to the wing. None changed the slope of the lift curve (fig. 14). The low nacelles 1A, 2B, and 2C caused the largest lift decreases. In order to maintain the required net lift coefficient, it would be necessary to increase the angle of attack of the wing, a procedure that would result in increased wing drag because of operation of the wing at higher than its design lift coefficient. In the design of the wing, therefore, the design lift coefficient should be determined from a consideration of the effects of nacelles and fuselage as well as of the wing loading.

#### PRESSURES AT WING-NACELLE JUNCTURE

The results shown in figure 17 are typical of all the nacelles tested. It will be noticed that the afterbodies of the so-called centrally located nacelles were larger on the under side of the wing than on the upper side because of the camber and the  $3^\circ$  angle of incidence of the wing. The pressures on the lower surface were thus disturbed to a greater extent than on the upper surface. As shown in figure 17, the local pressures became more negative on the lower surface at the wing-nacelle juncture than on the wing alone, whereas the upper-surface pressures became more positive. The contracting lines of the upper-surface junctures and the decreased circulation in the vicinity of the nacelle are probably jointly responsible for the reduced negative pressure peaks on the upper surface. This result is desirable because on a lifting wing the negative pressure peak on the upper surface determines the critical Mach number, and this peak should not be augmented by the presence of the nacelle. The pressure peak on the lower surface, even though increased by the nacelle, is not likely to exceed the upper-surface peak. (See fig. 17.) On the basis of these results, it is evident that none of the nacelle installations tested would reduce the critical speed below that of the wing.

Although no attempt was made to do so in the present tests, it appears possible to design a wing-nacelle junction that will not augment either the upper- or the lower-surface peaks.

### SUMMARY OF RESULTS

1. The minimum drags of conventional nacelles of various types and sizes installed on a 20.7-percent-thick low-drag wing were of the same order of magnitude as the minimum nacelle drags obtained in a previous investigation employing an 18-percent-thick conventional wing.

2. The estimated effect of the disturbance of the laminar boundary layer on the wing by the slipstream of a tractor propeller is to increase the nacelle drag from 12 to 21 percent, depending on the nacelle size.

3. The drag coefficients of nacelles that were unsatisfactory at low speeds increased very rapidly with increasing Mach number. For the best arrangements tested, however, no serious increases occurred within the limit of the tests, for which the highest Mach number was 0.55.

4. Decreases in nacelle size resulted in large drag reductions both through the reduced frontal area and through decreased interference effects.

5. A 60-inch-diameter pusher arrangement with provisions for handling all the air requirements of the Wright 3350 engine, but with no provision for housing a landing gear, had the lowest drag coefficient of any nacelle tested.

6. The minimum drags obtained with NACA cowlings C and E, as tested with the spinner stationary, were about equal at Mach numbers below 0.55. At higher angles of attack, cowling E had less drag and higher pressures available for cooling than cowling C.

7. Nacelles in the low position with the top of the nacelle flush with upper surface of wing had about the same drag as nacelles whose center lines passed through the trailing edge of wing, provided that the low afterbody was extended far enough beyond the trailing edge to prevent flow separation.

8. Low nacelles appeared to present less of a problem than central nacelles in designing for a high critical Mach number at the wing-nacelle juncture because only the relatively low local velocities on the under surface of the wing were augmented by the afterbody. With either the low or the central location it appears that the critical Mach number at the juncture can be made to exceed that of the wing alone by proper shaping of the nacelle afterbody.

9. The effect of air outlet through efficient openings resulted in reduced external drag in several cases. This effect was large enough to warrant further investigation. Nacelle-development programs should include tests to determine the most effective outlet location.

Langley Memorial Aeronautical Laboratory  
National Advisory Committee for Aeronautics  
Langley Field, Va.

#### REFERENCES

1. Robinson, Russell G., and Becker, John V.: High-Speed Tests of Conventional Radial-Engine Cowlings. NACA Rep. No. 745, 1942.
2. Becker, John V.: Wind-Tunnel Tests of Air Inlet and Outlet Openings on a Streamline Body. NACA ACR, Nov. 1940.
3. Wilson, Herbert A., Jr., and Lehr, Robert R.: Drag and Propulsive Characteristics of Air-Cooled Engine-Nacelle Installations for Two-Engine Airplanes. NACA ACR, Dec. 1940.

TABLE I. - continued

NACELLE ORDINATES IN INCHES - continued

TABLE I. NACELLE ORDINATES IN INCHES  
[See figs. 1 and 2]

Manufacturer's original nacelle					
x	y <sub>U</sub>	x	y <sub>L</sub>	x	y <sub>B</sub>
0	3.650	0	3.065	0	3.36
.011	3.676	.024	3.125	.018	3.383
.030	3.713	.055	3.184	.043	3.450
.066	3.765	.116	3.273	.093	3.523
.141	3.846	.240	3.405	.193	3.631
.289	3.959	.489	3.590	.394	3.783
.438	4.039	.736	3.731	.594	3.894
.587	4.106	.990	3.841	.794	3.984
.734	4.166	1.233	3.940	.995	4.064
.883	4.213	1.481	4.023	1.195	4.133
1.105	4.278	1.853	4.139	1.495	4.216
1.475	4.361	2.474	4.280	1.998	4.331
1.845	4.428	3.093	4.380	2.498	4.420
2.216	4.475	3.711	4.451	2.998	4.480
2.639	4.500	4.421	4.500	3.570	4.500
6.550	4.500	6.550	4.500	6.550	4.500
6.550	4.120	6.550	4.120	6.550	4.120
7.050	4.330	7.050	4.330	7.050	4.330
8.250	4.500	8.250	4.500	8.250	4.500
12.060	4.500	12.060	4.500	12.060	4.500
17.220		17.220	4.270	17.220	4.420
22.060		22.060	3.350	22.060	4.010
27.060		27.060	1.110	27.060	2.270
30.620		30.620	0	30.620	0

NACELLE 1		NACELLE 1A					
x	y (radius)	x	y (radius)	x	y <sub>U</sub>	y <sub>L</sub>	y <sub>B</sub>
0	3.15	0	3.15	12.06	4.48	4.48	4.48
.043	3.40	.043	3.40	16.45	4.48	4.30	4.30
.086	3.48	.086	3.48	21.95	----	3.73	3.73
.173	3.59	.173	3.59	27.95	----	2.30	2.30
.346	3.75	.346	3.75	30.54	1.49	1.50	1.50
.519	3.88	.519	3.88	31.50	1.28	1.11	1.09
.692	3.97	.692	3.97	32.47	1.00	.72	.62
.865	4.07	.865	4.07	33.06	.77	.47	.33
1.039	4.14	1.039	4.14	33.66	0	0	0
1.210	4.21	1.210	4.21				
1.383	4.27	1.383	4.27				
1.73	4.37	1.73	4.37				
2.08	4.44	2.08	4.44				
2.42	4.48	2.42	4.48				
2.77	4.50	2.77	4.50				
6.55	4.50	6.55	4.50				
6.55	4.12	6.55	4.12				
7.05	4.33	7.05	4.33				
8.25	4.50	8.25	4.50				
13.50	4.50						
16.50	4.37						
18.50	4.13						
20.50	3.75						
22.50	3.21						
24.50	2.56						
26.50	1.83						
28.50	.98						
30.62	0						

TABLE I. - continued  
NACELLE ORDINATES IN INCHES - continued

TABLE I. - continued  
NACELLE ORDINATES IN INCHES - continued

NACELLE 2					
x	y (radius)	x	y <sub>U</sub>	y <sub>L</sub>	y <sub>s</sub>
0	1.78	4.75	3.86	3.86	3.50
.018	1.84	5.75	4.20	4.20	3.67
.032	1.87	7.00	4.43	4.43	3.86
.050	1.89	8.00	4.50	4.50	4.00
.068	1.91	9.88	4.50	4.50	4.20
.095	1.94	9.88	4.50	4.50	3.67
.130	1.98	12.00	4.50	4.50	4.23
.194	2.03	14.75	4.50	4.50	4.50
.320	2.13	16.00	4.50	4.50	4.50
.643	2.32	16.00	3.65	4.50	4.50
.968	2.48	18.00	4.02	4.48	4.48
1.29	2.61	20.00	4.10	4.37	4.37
1.93	2.84	22.00	4.03	4.13	4.13
2.57	3.02	24.00	3.75	3.75	3.75
3.21	3.18	26.00	3.21	3.21	3.21
3.75	3.31	28.00	2.56	2.56	2.56
		30.00	1.82	1.82	1.82
		32.00	.98	.98	.98
		34.05	0	0	0

NACELLE 3			NACELLE 4			NACELLE 5		
x	y <sub>U,L</sub>	y <sub>s</sub>	x	y (radius)	y <sub>s</sub>	x	R <sub>0</sub>	R <sub>I</sub>
0	2.30	3.15	0	2.537		0	1.78	1.78
.043	2.55	3.40	.035	2.739		.050	1.89	1.75
.086	2.63	3.48	.070	2.802		.095	1.94	1.75
.173	2.74	3.59	.139	2.893		.130	1.98	1.76
.346	2.90	3.75	.279	3.018		.320	2.13	1.77
.518	3.03	3.88	.418	3.123		.643	2.32	1.80
.692	3.12	3.97	.558	3.199		.968	2.48	1.83
.865	3.22	4.07	.697	3.276		1.29	2.61	1.85
1.039	3.29	4.14	.836	3.332		1.93	2.84	1.88
1.210	3.36	4.21	.976	3.387		2.50	2.96	1.92
1.38	3.42	4.27	1.115	3.436		3.00	3.08	1.95
1.73	3.52	4.37	1.394	3.520		4.00	3.27	2.17
2.08	3.59	4.44	1.673	3.576		5.00	3.41	2.60
2.42	3.63	4.48	1.952	3.610		6.00	3.52	2.97
2.77	3.65	4.50	2.230	3.625		7.00	3.60	3.20
3.37	3.65	4.50	2.251	3.625		8.00	3.66	3.37
6.625	3.65	4.50	2.426	3.625		10.00	3.71	3.52
6.625	3.65	3.85	6.625	3.625	3.625	12.00	3.75	
7.625	3.65	4.12	6.625	3.625	2.930	14.00	3.75	
8.625	3.65	4.35	7.625	3.625	3.250	16.00	3.69	
10.000	3.65	4.45	8.625	3.625	3.450	18.00	3.55	
10.000	3.05	4.45	10.000	3.580	3.580	20.00	3.31	
11.500	3.20	4.40	14.000	3.450		22.00	2.96	
14.000	3.45	4.28	18.000	3.130		24.00	2.50	
18.000	3.13	3.89	20.000	2.850		25.75	2.00	
22.000	2.49	3.09	22.000	2.490		25.75	1.68	
26.000	1.47	1.83	26.000	1.470		26.25	1.57	
30.625	0	0	30.625	0		27.00	1.36	
						28.00	1.00	
						29.00	.61	
						30.05	0	

Nacelle 3B (1)			
x	y <sub>U</sub>	y <sub>L</sub>	y <sub>s</sub>
10.00	3.05	3.58	4.45
11.50	3.20	3.45	4.40
14.00	3.45	3.10	3.85
18.00	3.13	2.05	2.54
20.50		1.20	

<sup>1</sup>Ordinates forward of 10-inch station same as nacelle 3.

TABLE II  
DRAG OF NACELLES TESTED

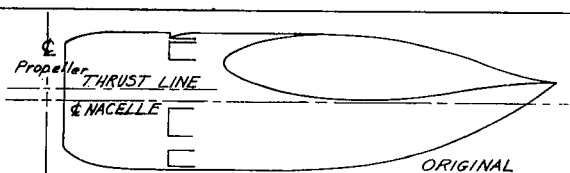
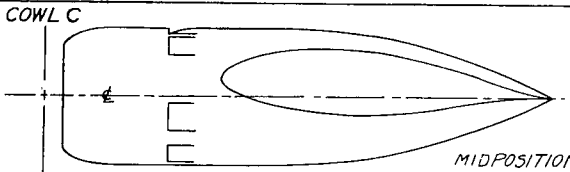
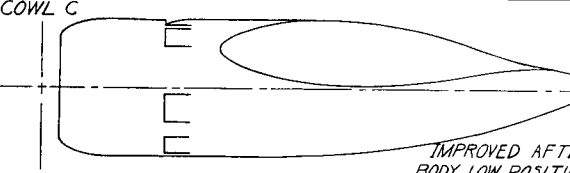
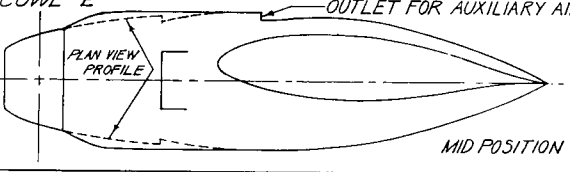
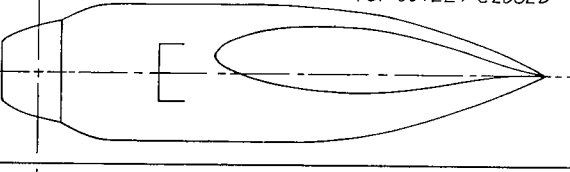
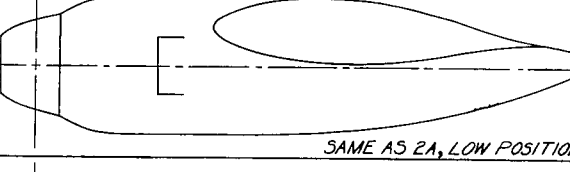
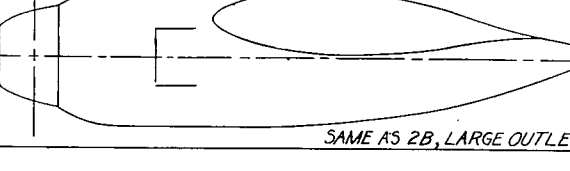
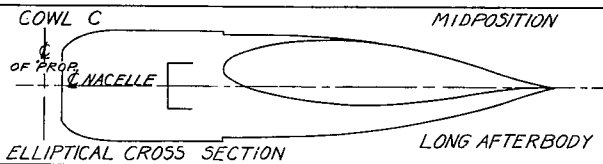
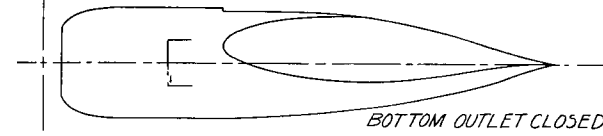
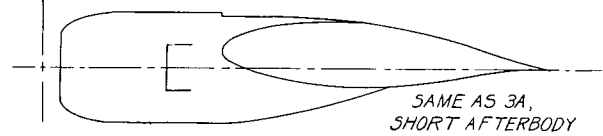
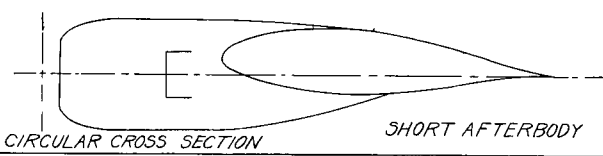
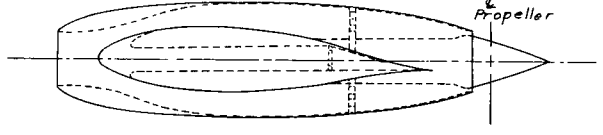
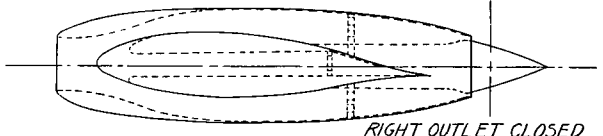
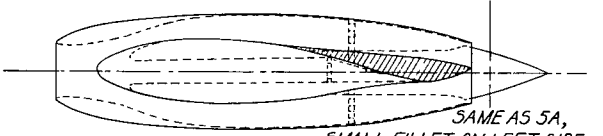
MODEL ARRANGEMENT		INTERNAL FLOW PO PABV	$M=0.5 \quad \alpha=2^\circ$	
			$C_{DF}$	EXT. DRAG AT 25,000 FT (lb)
	 <p>Propeller THRUST LINE NACELLE ORIGINAL NACELLE</p>	0.051	0.174	680
1	 <p>COWL C MID POSITION</p>	.051	.085	335
1A	 <p>COWL C IMPROVED AFTER- BODY, LOW POSITION</p>	.051	.080	315
2	 <p>COWL E OUTLET FOR AUXILIARY AIR PLAN VIEW PROFILE MID POSITION</p>	.118	.061	240
2A	 <p>TOP OUTLET CLOSED</p>	.053	.088	345
2B	 <p>SAME AS 2A, LOW POSITION</p>	.053	.088	345
2C	 <p>SAME AS 2B, LARGE OUTLETS</p>	.074	.090	350

TABLE II.-Concluded.  
DRAG OF NACELLES TESTED - Continued.

MODEL ARRANGEMENT		INTERNAL FLOW $\frac{P_0}{P_\infty}$ $\frac{P_0}{P_\infty} \frac{A_0}{A}$	$M=0.5 \quad \alpha=2^\circ$	
			$C_{DF}$	EXT. DRAG AT 25,000 FT (lb)
3	 <p>COWL C OF PROP NACELLE ELLIPTICAL CROSS SECTION MIDPOSITION LONG AFTERBODY</p>	0.126	0.056	180
3A	 <p>BOTTOM OUTLET CLOSED</p>	.093	<sup>a</sup> .054	—
3B	 <p>SAME AS 3A, SHORT AFTERBODY</p>	.093	.061	200
4	 <p>CIRCULAR CROSS SECTION SHORT AFTERBODY</p>	.065	.053	145
5	 <p>Propeller</p>	.113	.040	110
5A	 <p>RIGHT OUTLET CLOSED</p>	.089	.052	140
5B	 <p>SAME AS 5A, SMALL FILLET ON LEFT SIDE</p>	.089	.045	120

<sup>a</sup> For  $M=0.3$ .

N.F.S. 8'H.S.T.  
10-1-71

TABLE III  
INTERNAL-DRAG INCREMENTS  
[ $\alpha = 2^\circ$ ;  $M = 0.50$ ]

Nacelle	Flow condition	$\Delta C_{DF}$
Original	Engine cooling air only	0.006
1	. . . . . do . . . . .	.006
1A	. . . . . do . . . . .	.006
2	Complete air requirements	.020
2A	Engine cooling air only	.011
2B	. . . . . do . . . . .	.011
2C	Enlarged side outlets	.023
3	Complete air requirements	.024
3A	Bottom outlet closed	.010
3B	. . . . . do . . . . .	.010
3C	Auxiliary air only	.003
3D	Engine cooling air only	.003
4	1.25 X engine cooling air	.016
5	Complete air requirements	.017
5A	Right outlet closed	.014
5B	. . . . . do . . . . .	.014
5C	Left outlet closed	.014



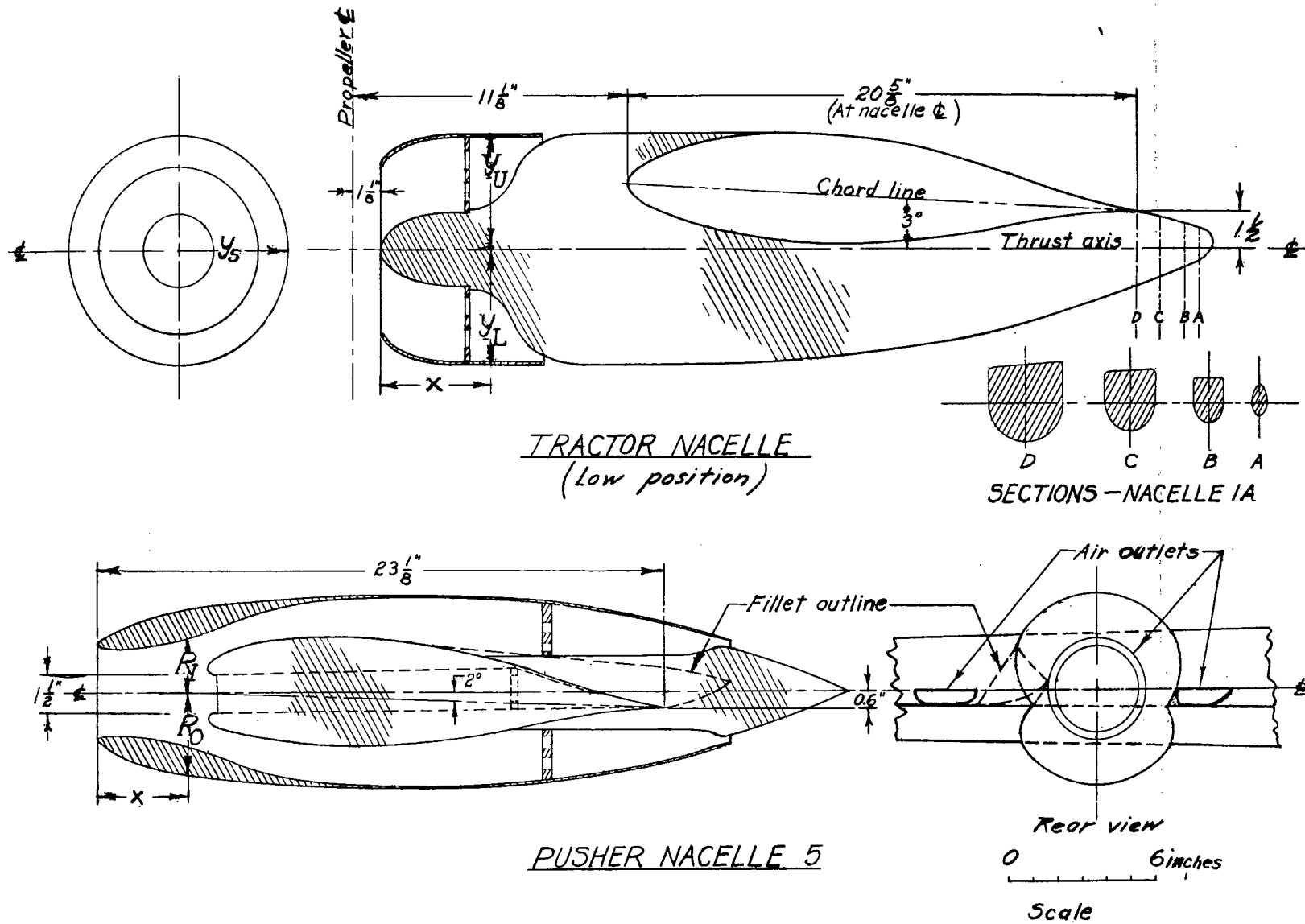


Figure 1.- General arrangement of nacelles.

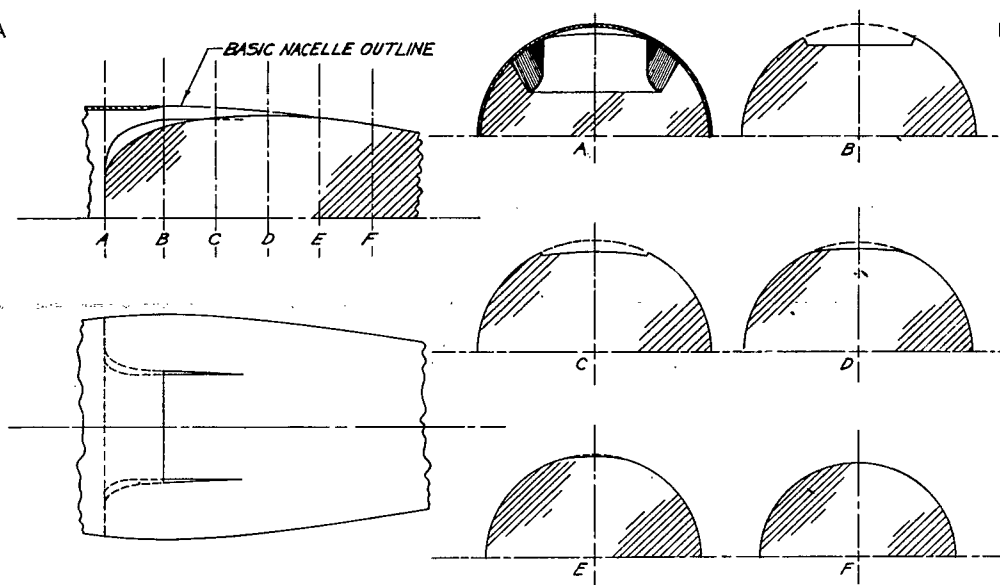


FIGURE 2 - TYPICAL AIR OUTLET.  
(TOP OUTLET, NACELLE 2)

0 6"  
SCALE

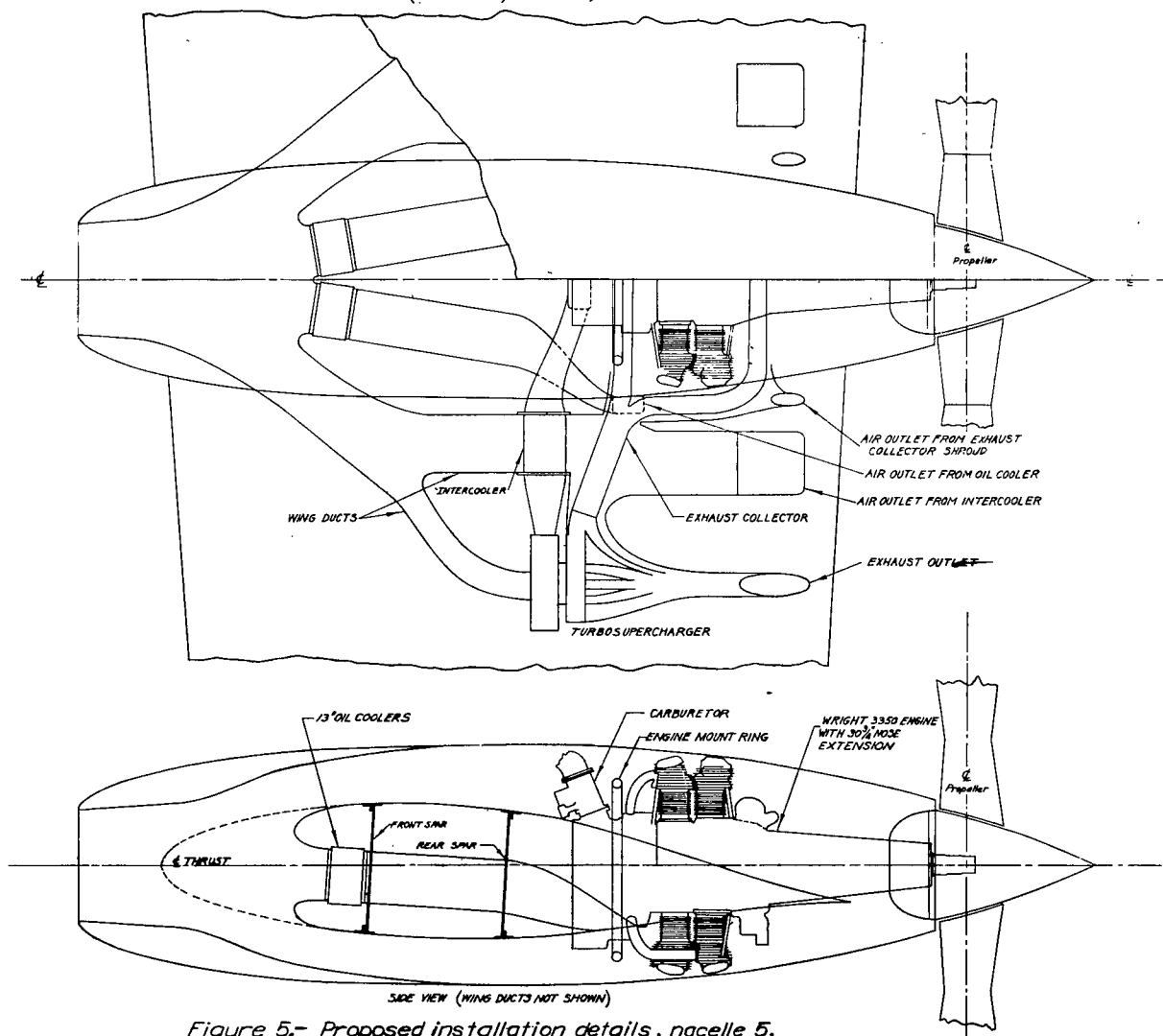


Figure 5.- Proposed installation details, nacelle 5.

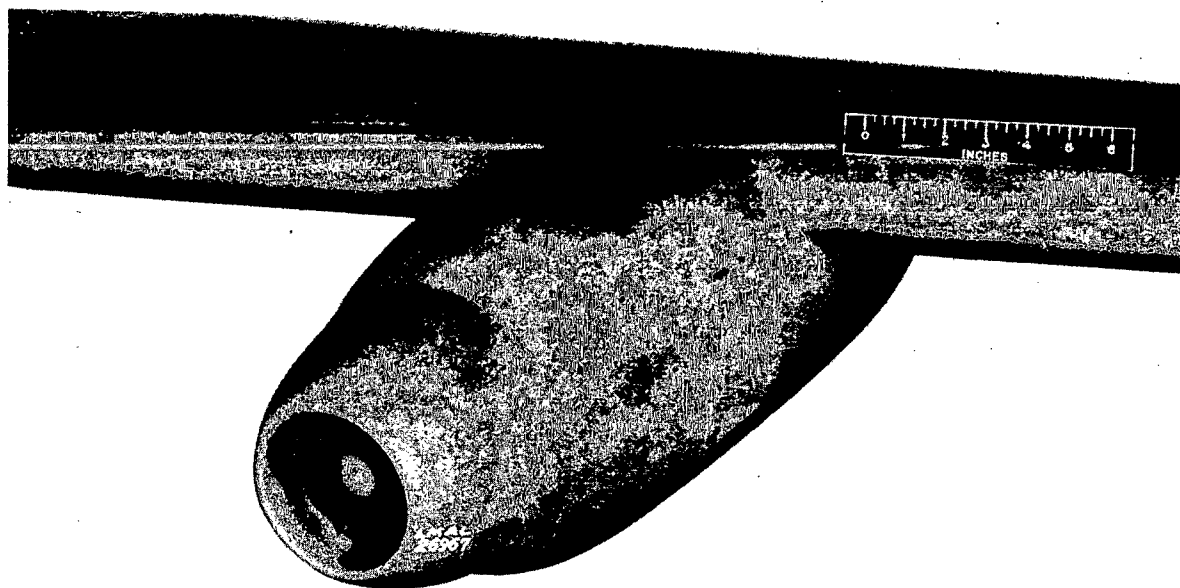


Figure 3a.- Nacelle 2C. Three quarter view.

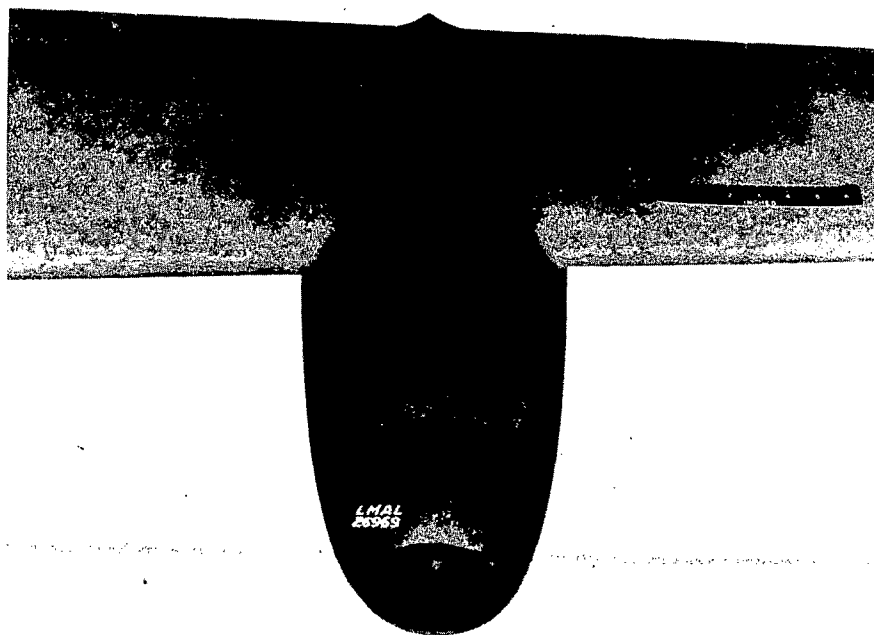


Figure 3b.- Nacelle 2C. Top view.

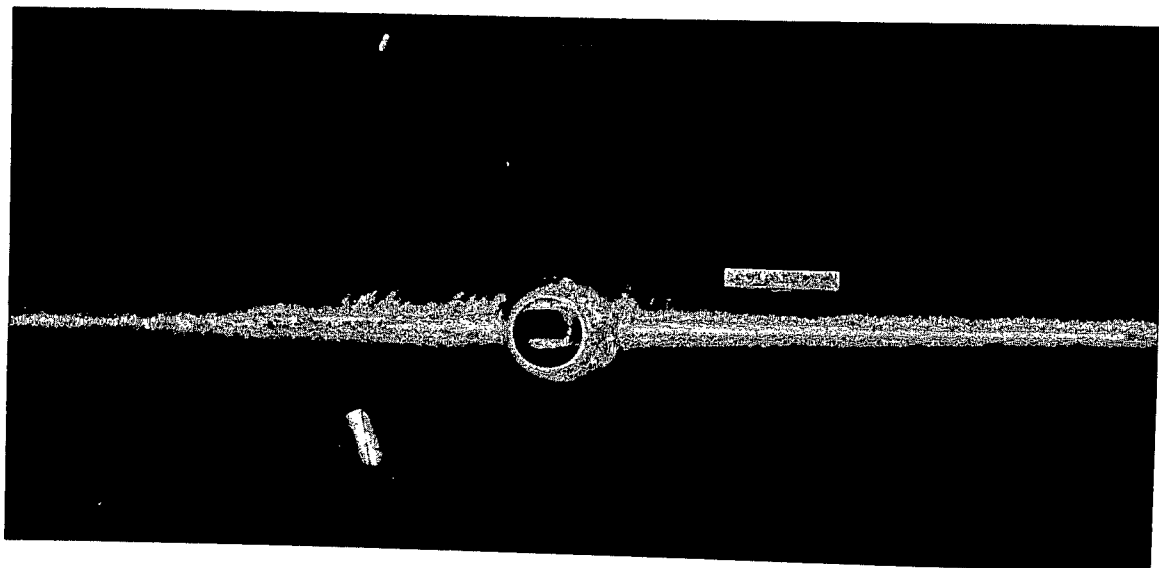


Figure 4a.- Nacelle 5. Front view.

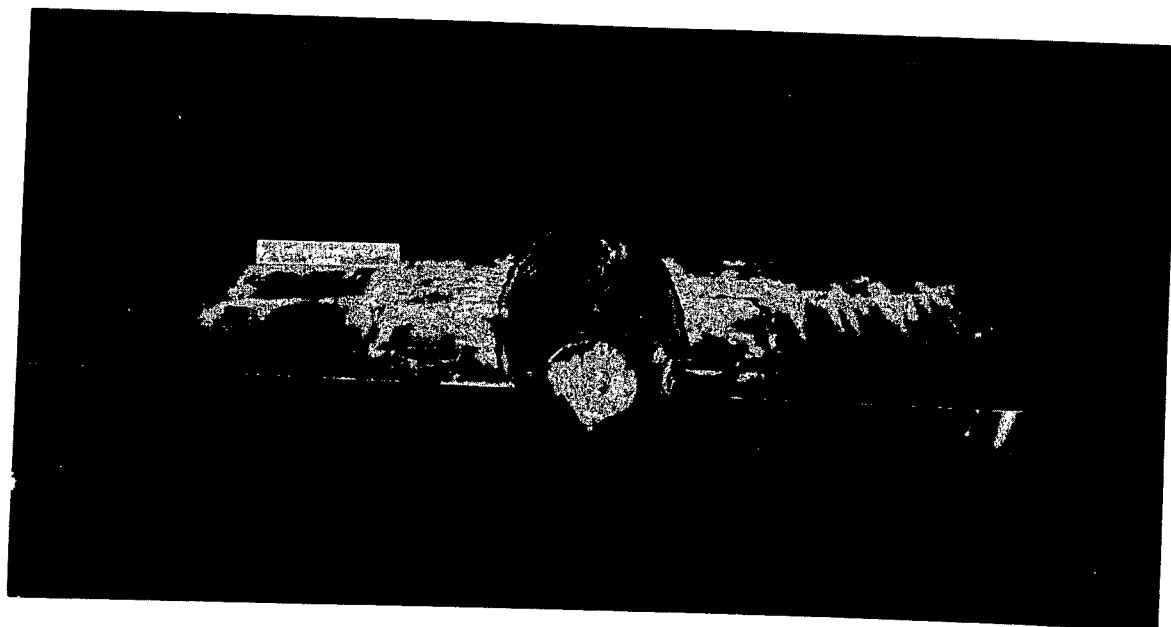
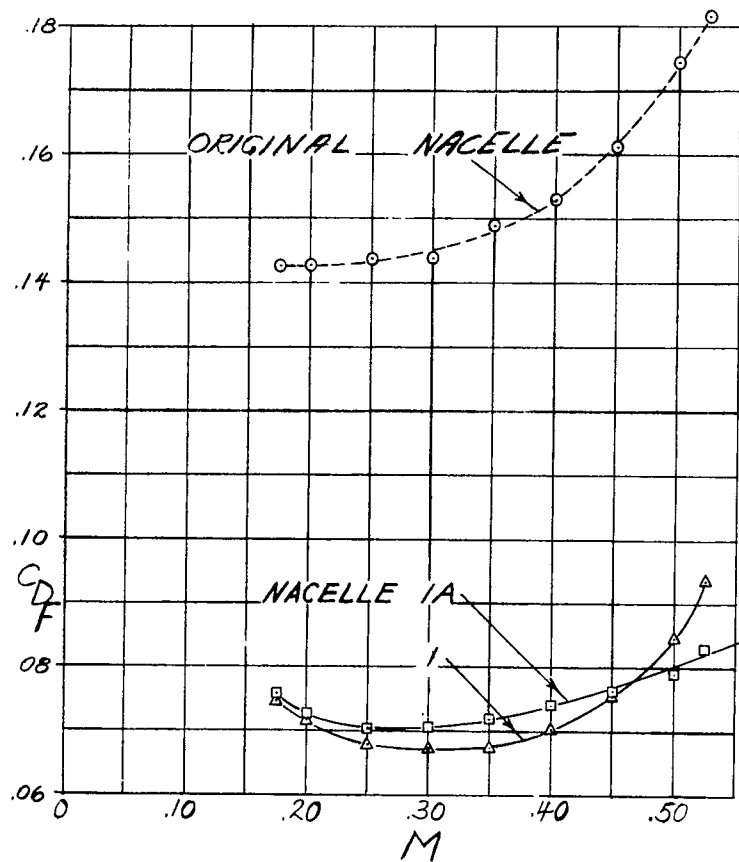
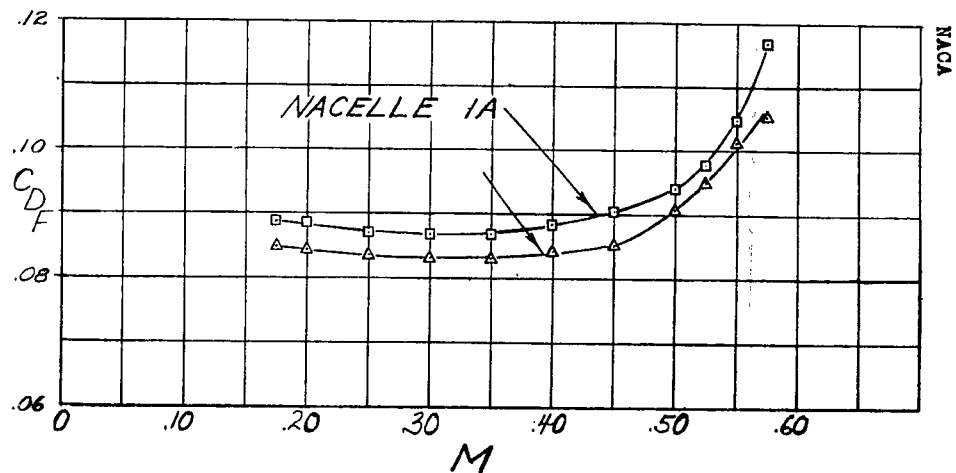


Figure 4b.- Nacelle 5. Rear view.

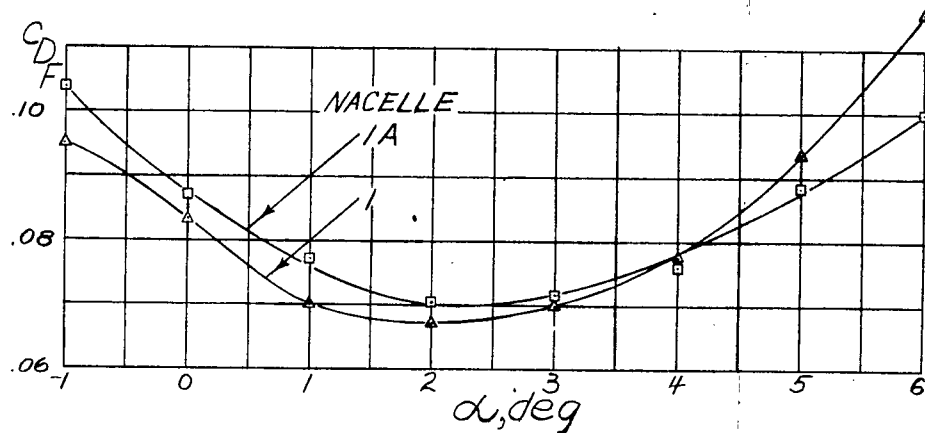


(a) Variation of drag with Mach number;  $\alpha = 2^\circ$ .  
Figure 6.- Characteristics of the 72-inch-diameter  
nacelles; conventional cowl.

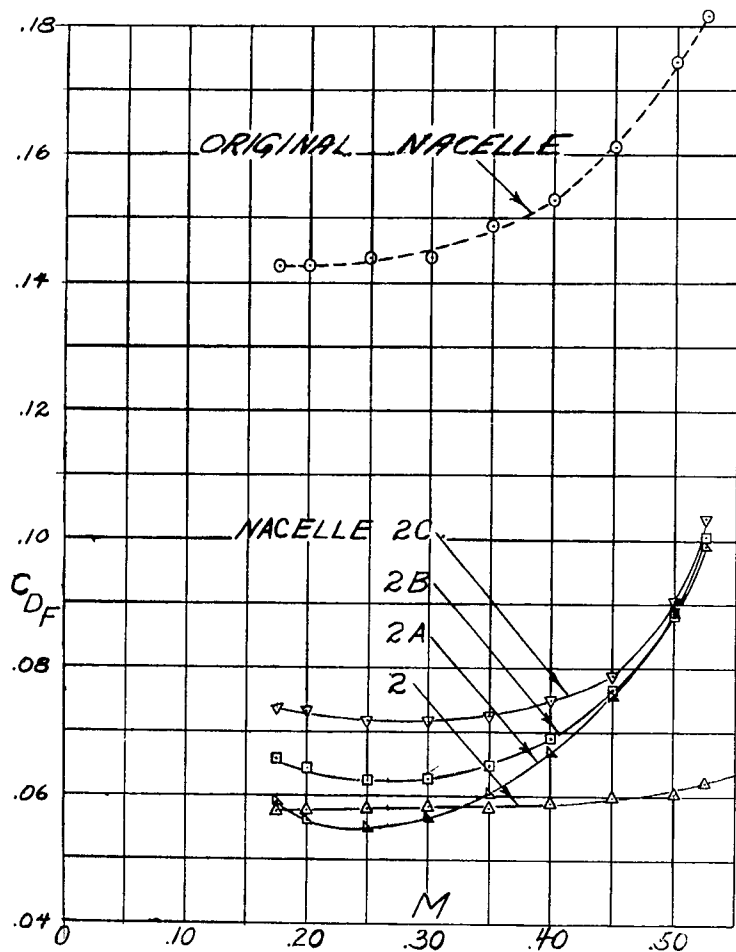


(b) Variation of drag with Mach number;  $\alpha = 0^\circ$ .

Figure 6.-Continued.

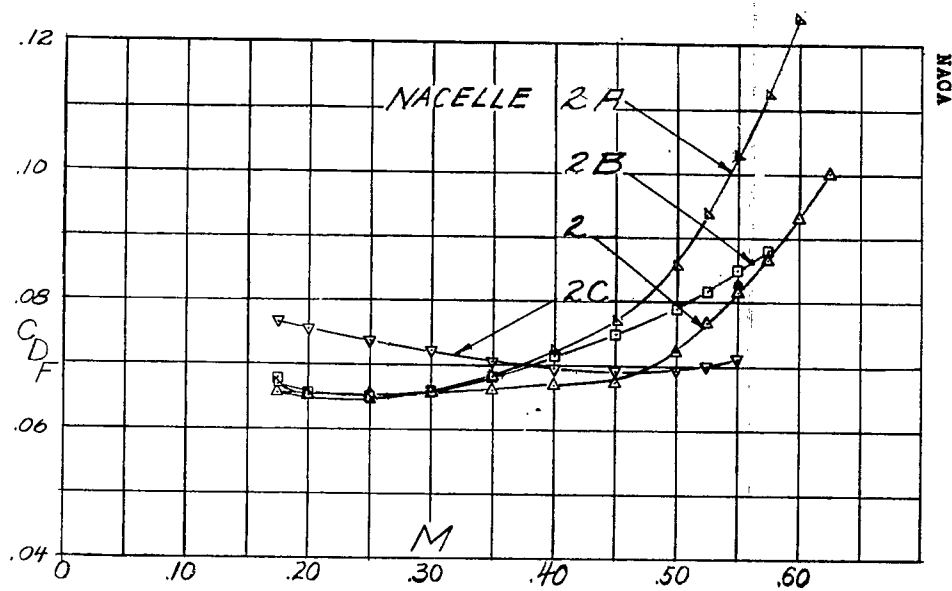


(c) Variation of drag with angle of attack;  $M = 0.28$   
Figure 6.- Concluded.



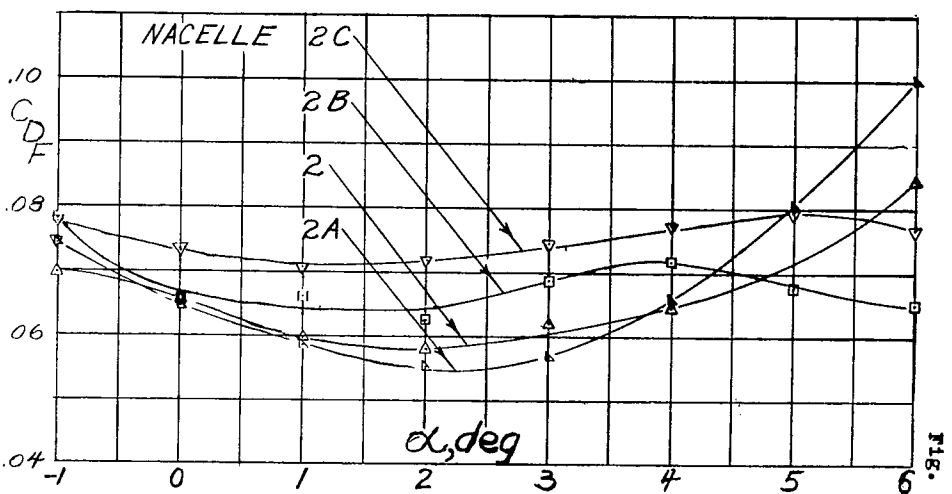
(a) Variation of drag with Mach number;  $\alpha = 2^\circ$ .

Figure 7.- Characteristics of the 72-inch-diameter nacelles; NACA cowling E.



(b) Variation of drag with Mach number;  $\alpha = 0^\circ$ .

Figure 7.- Continued.



(c) Variation of drag with angle of attack;  $M = 0.26$ .

Figure 7.- Concluded.

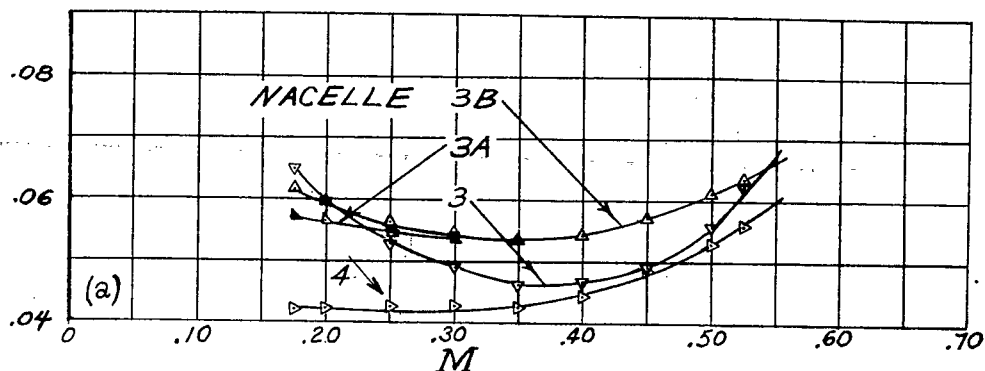


Figure 8.- Characteristics of the 72- by 60-inch elliptical and the 60-inch-diameter nacelles, NACA cowling C.

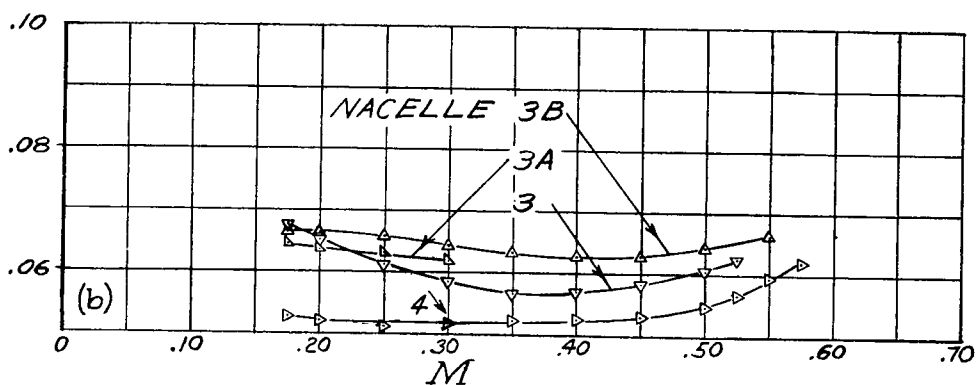


Figure 8.- Continued.

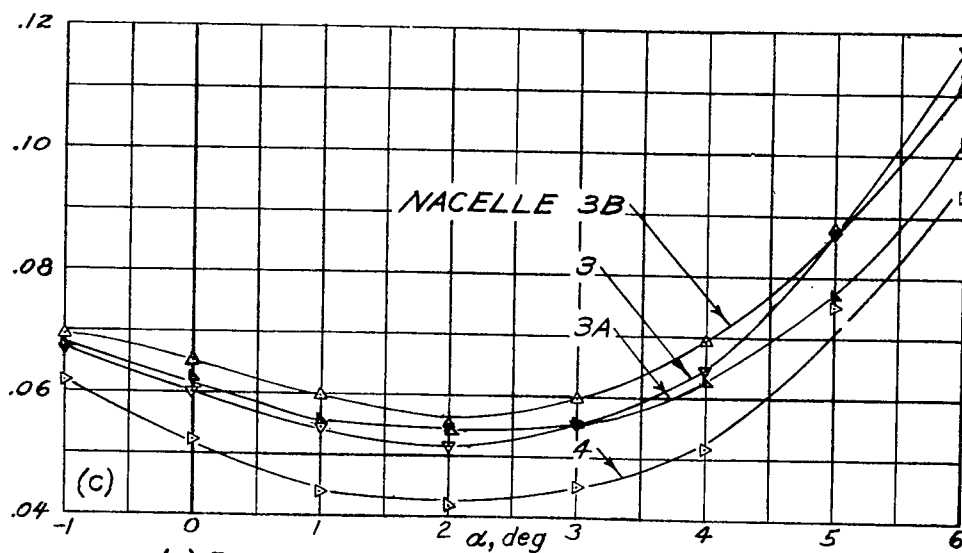
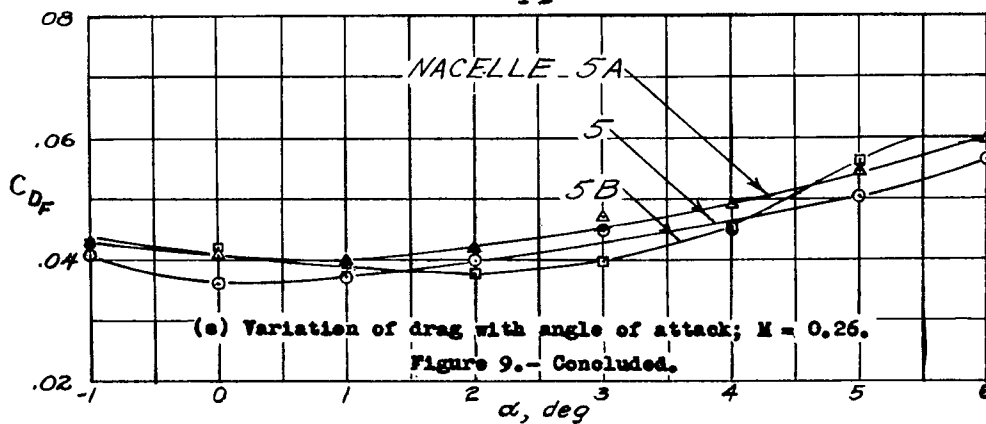
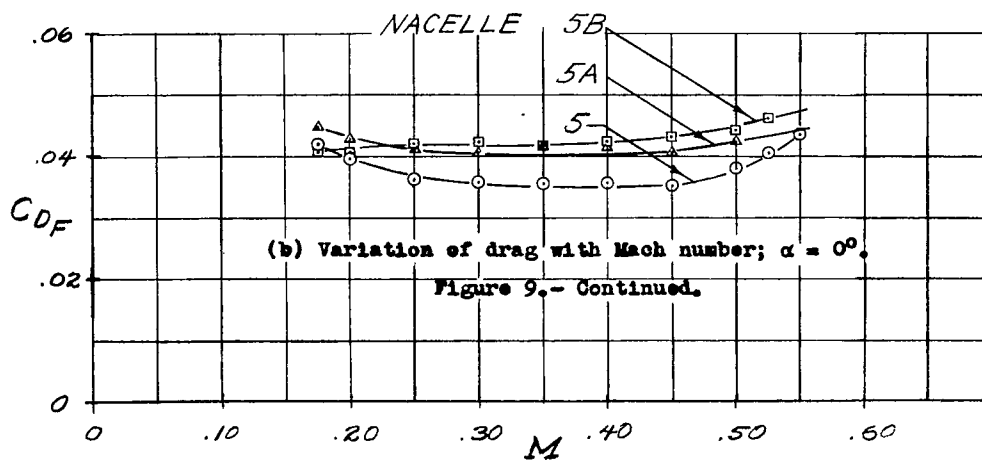
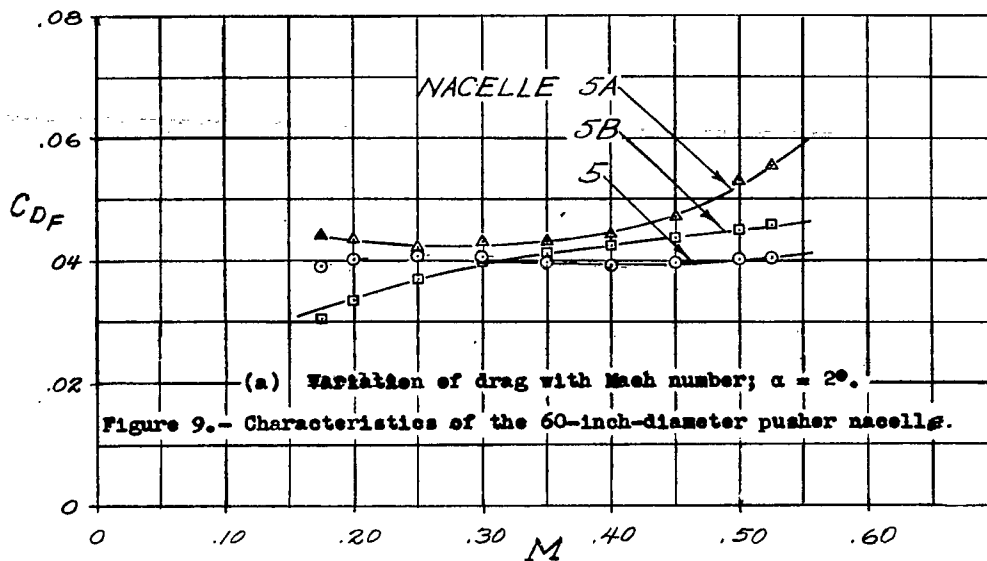
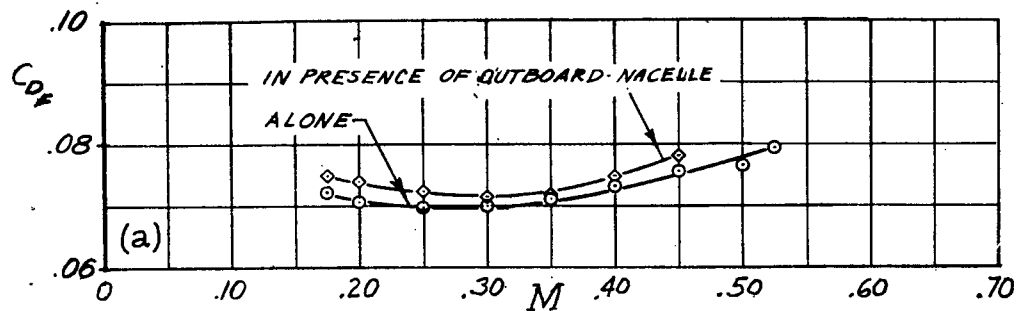


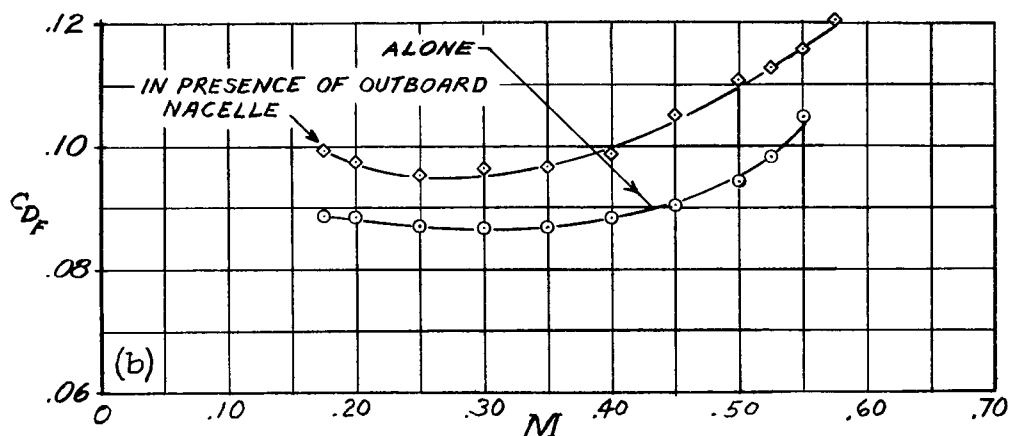
Figure 8.- Concluded.



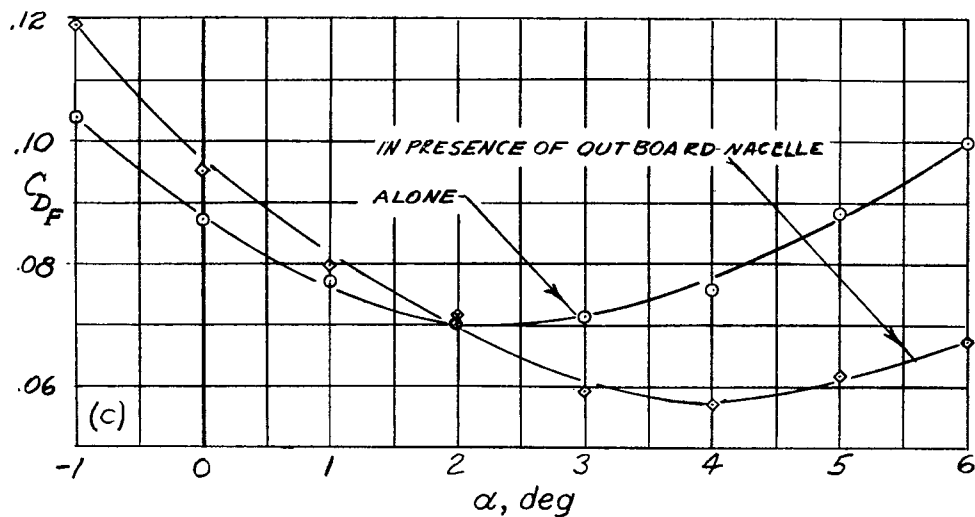




(a) Variation of drag with Mach number;  $\alpha = 2^\circ$ .  
 Figure 10.- Interference between inboard and outboard nacelles. Nacelle 1A.



(b) Variation of drag with Mach number;  $\alpha = 0^\circ$ .  
 Figure 10.- Continued.



(c) Variation of drag with angle of attack;  $M = 0.26$ .  
 Figure 10.- Concluded.

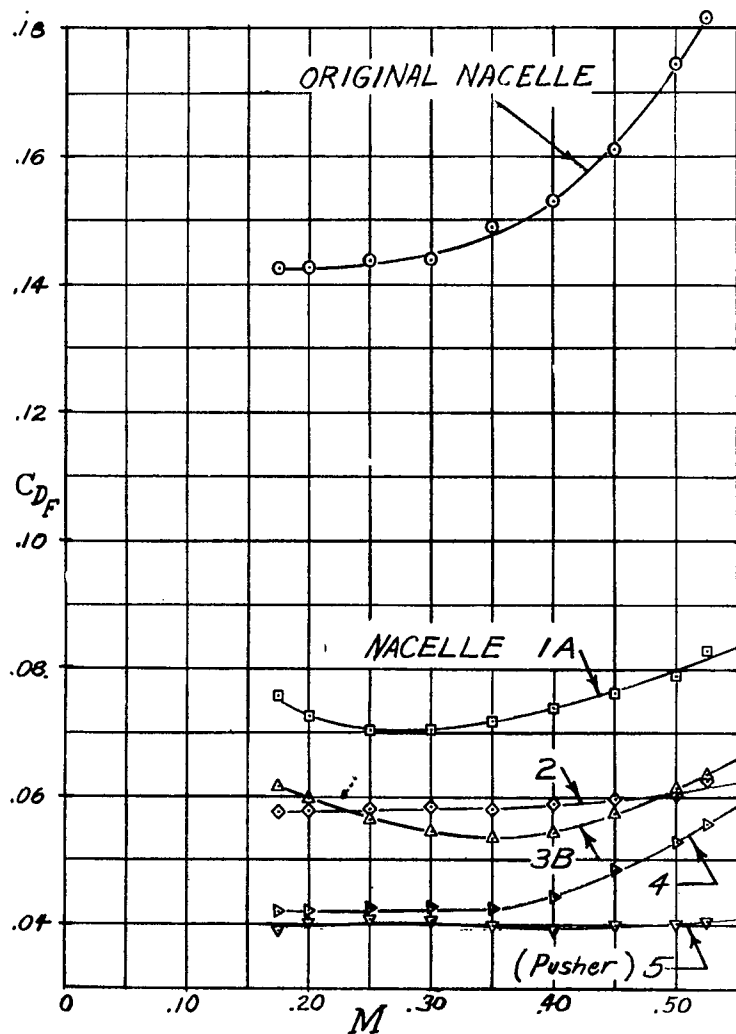


Figure 11.- Comparison of the drag coefficients of typical nacelle arrangements.  $\alpha = 2^\circ$ .

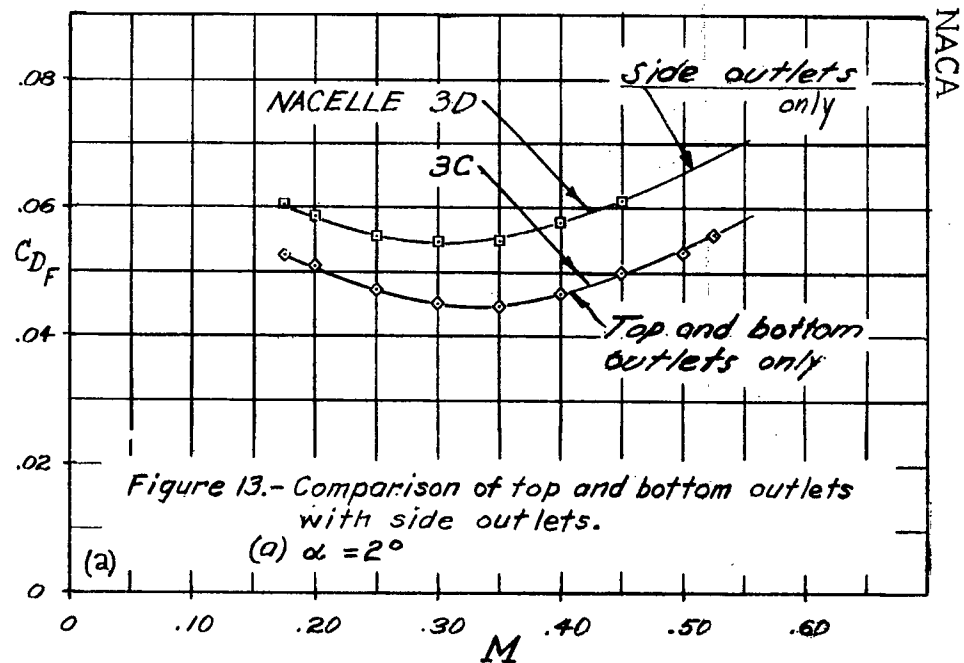


Figure 13.- Comparison of top and bottom outlets with side outlets.

(a)  $\alpha = 2^\circ$

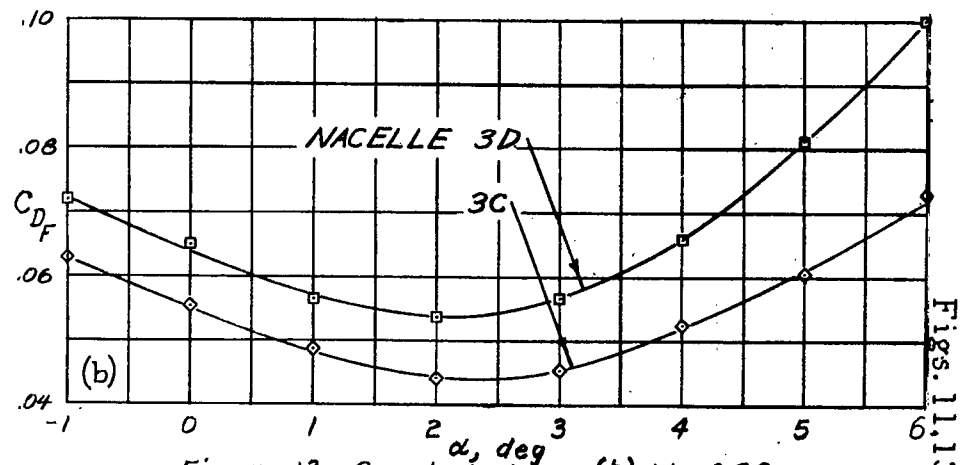


Figure 13.- Concluded. (b)  $M = 0.26$ .

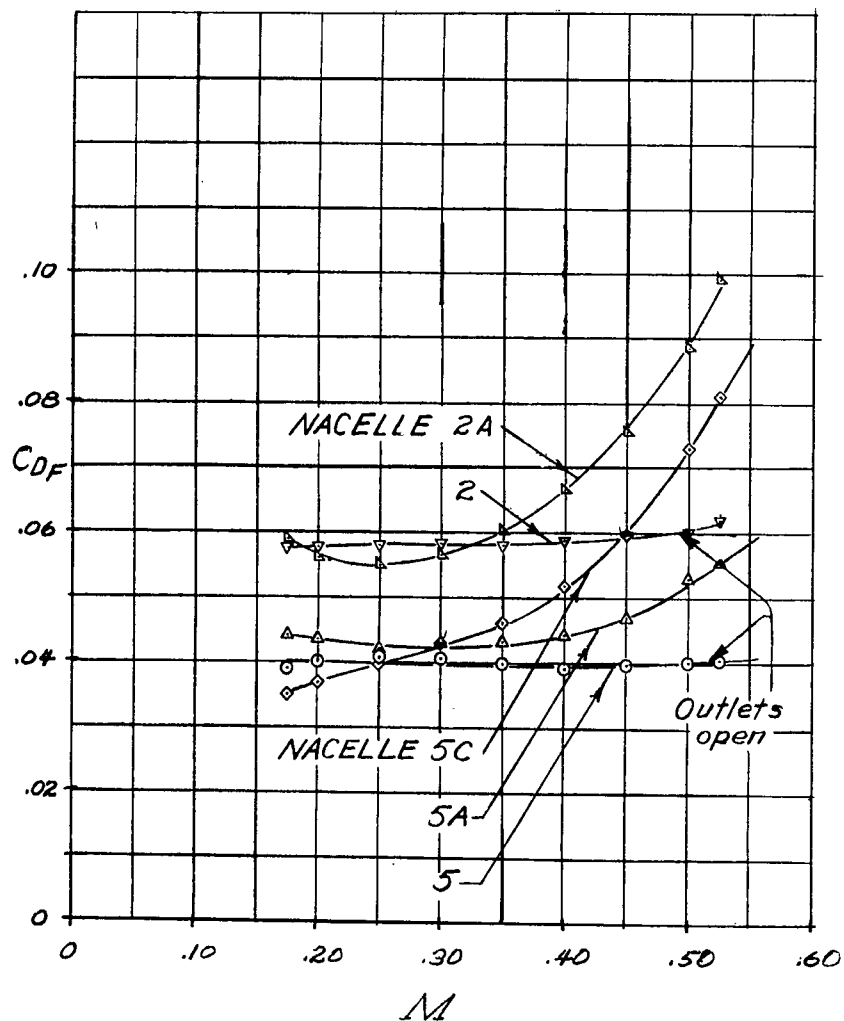


Figure 12.- Beneficial effects of air outlets on nacelle drag.  
(a)  $\alpha = 2^\circ$ .

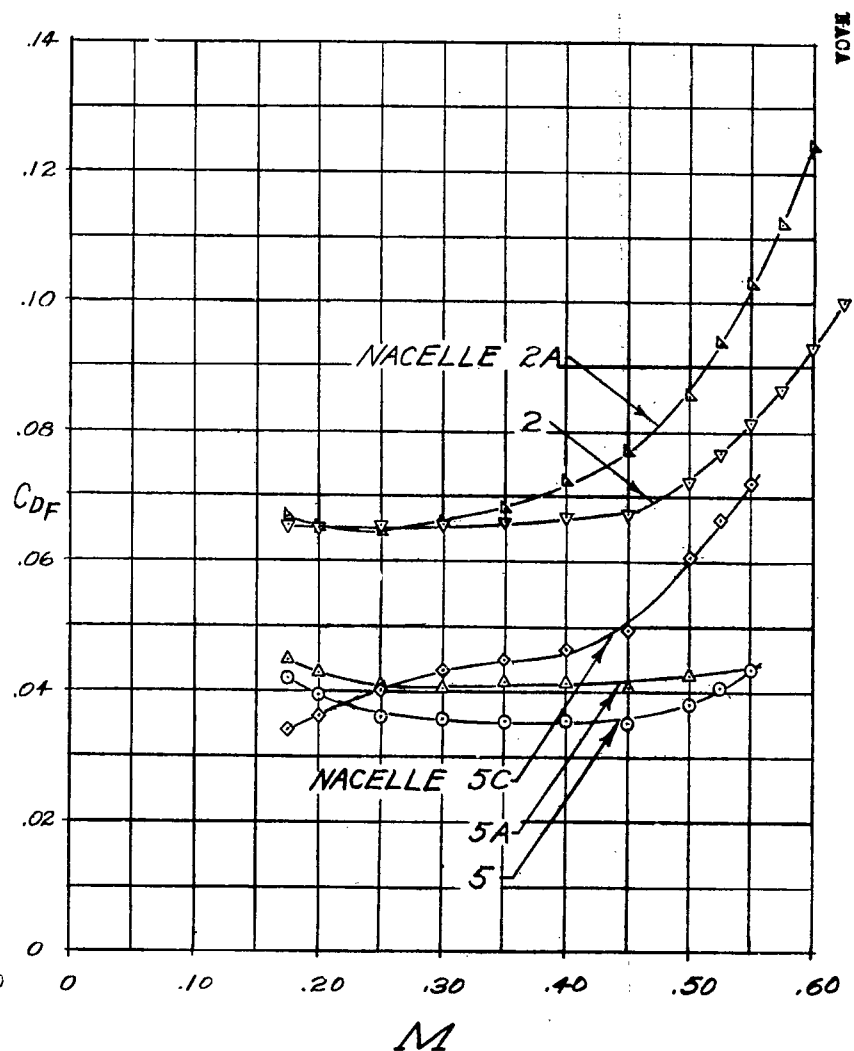


Figure 12.- Concluded.  
(b)  $\alpha = 0^\circ$ .

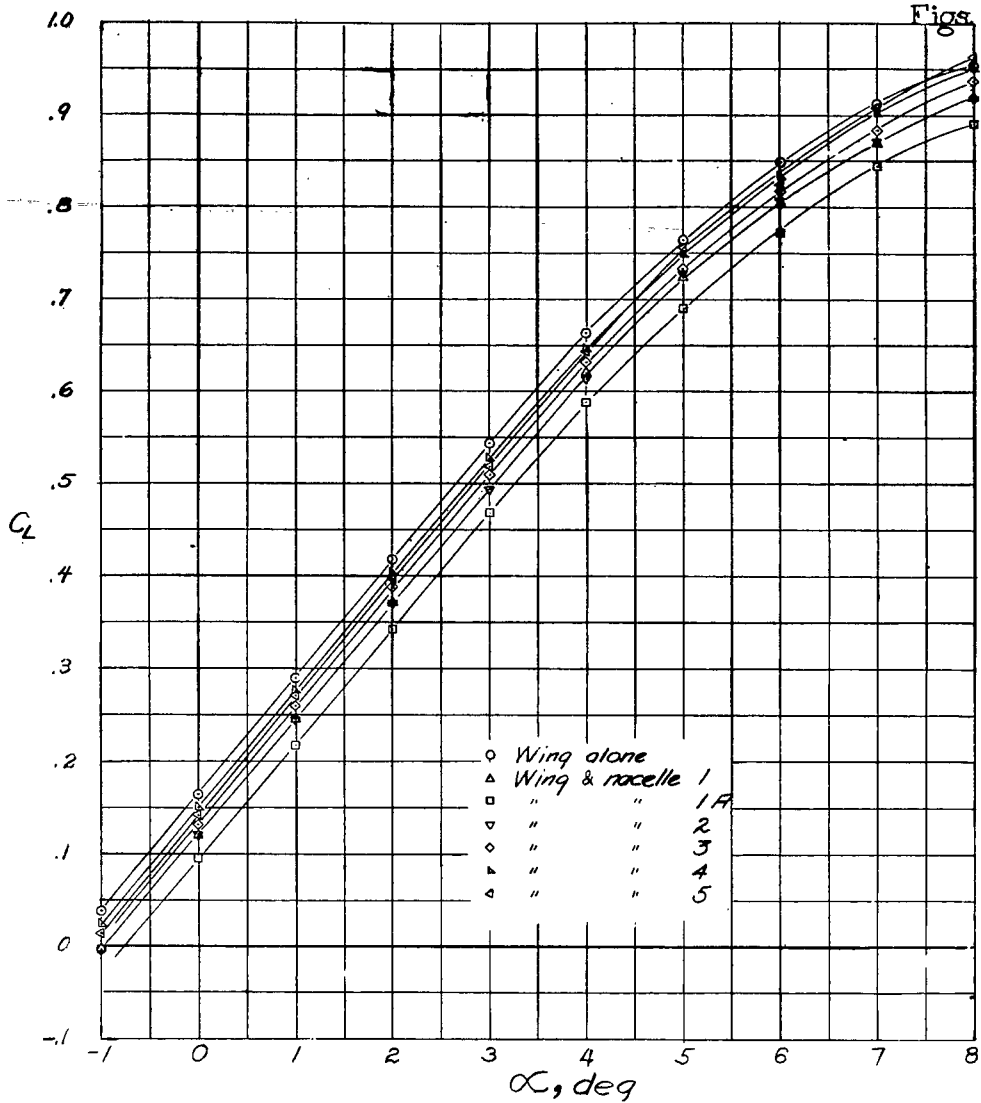


Figure 14.- The effect of the nacelles on the lift characteristics.  $M = 0.26$

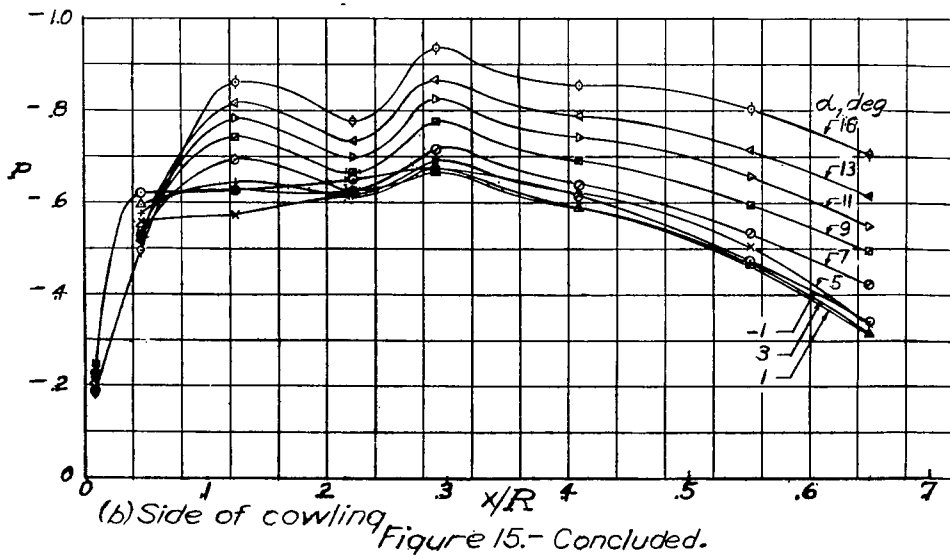


Figure 15.- Concluded.

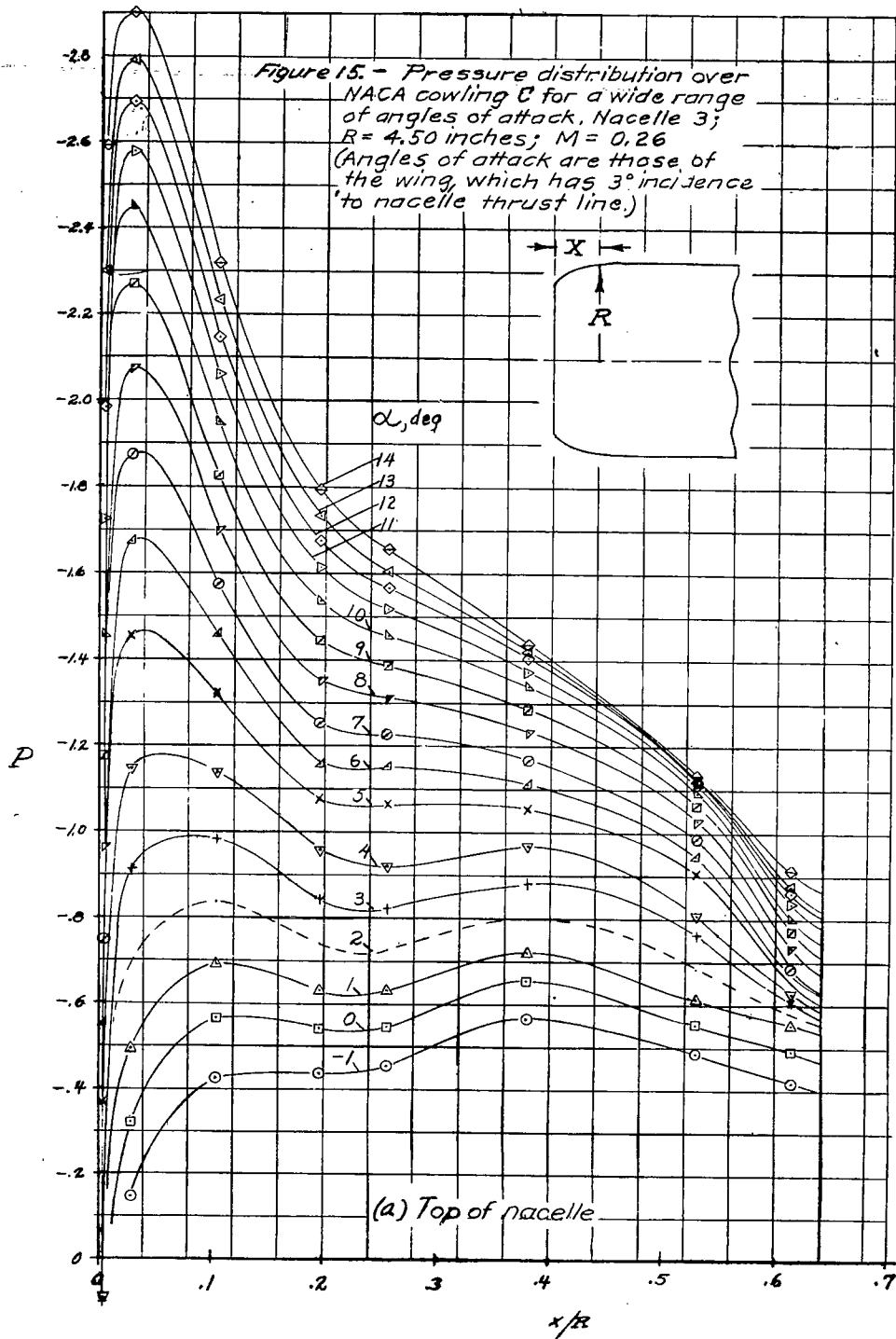


Figure 16.- Variation with Mach number of the pressure coefficient at  $x/R=0.104$ .  
Peak pressure station at  $\alpha=2^\circ$  and  $3^\circ$ ;  
Nocelle 3; NACA cowl C;  $R=4.50$  inches.

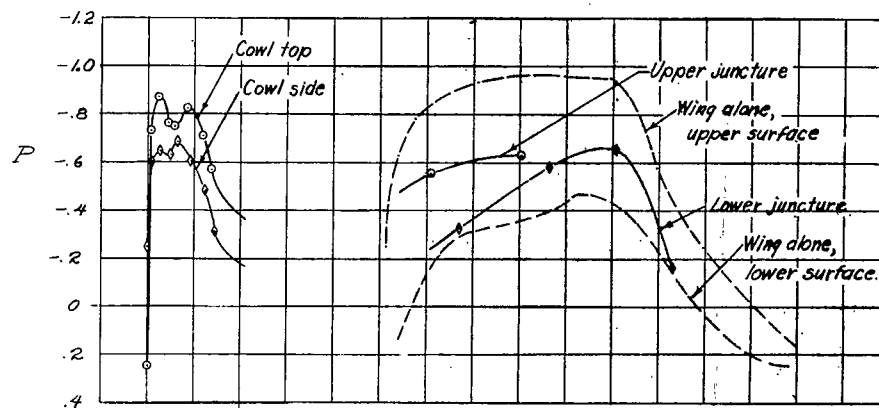
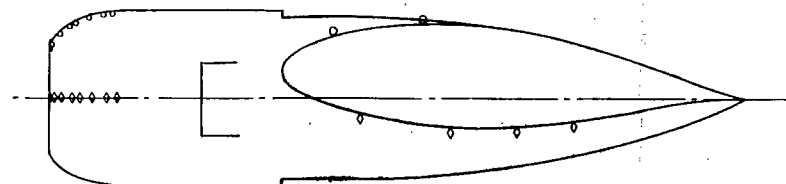
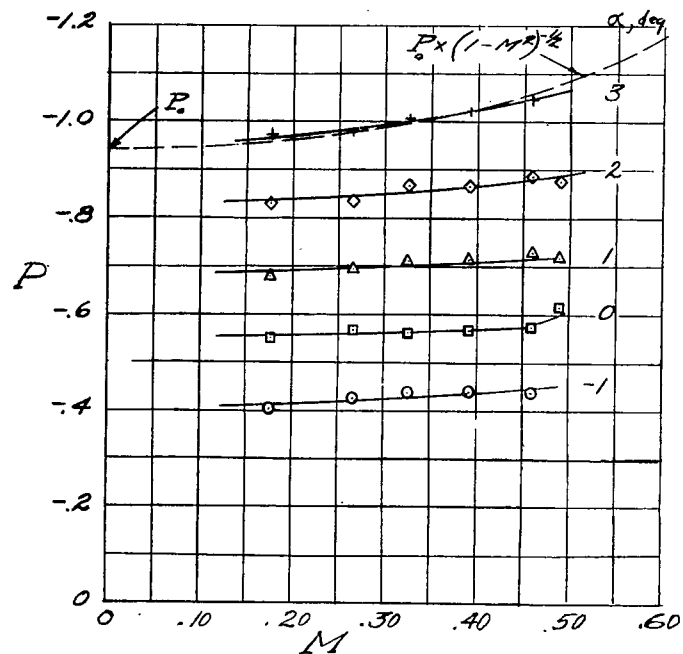


Figure 17.- Typical pressure distribution at wing-nocelle juncture. Nocelle 3;  $C_L=0.39$ ;  $M=0.26$ .

613

LANGLEY RESEARCH CENTER



3 1176 01354 2197